ADAPTIVE CAMERA TAMPER DETECTION FOR VIDEO SURVEILLANCE

A THESIS SUBMITTED TO
THE GRADUATE SCHOOL OF INFORMATICS
OF
THE MIDDLE EAST TECHNICAL UNIVERSITY

BY

ALİ SAĞLAM

IN PARTIAL FULFILLMENT OF THE REQUIREMENTS FOR THE DEGREE OF
MASTER OF SCIENCE
IN
THE DEPARTMENT OF INFORMATION SYSTEMS

JUNE 2009

Approval of the Graduate School of Informatics

_____

Prof. Dr. Nazife Baykal

Director

I certify that this thesis satisfies all the requirements as a thesis for the degree of Master of Science.

_____

Prof. Dr. Yasemin Yardımcı

Head of Department

This is to certify that we have read this thesis and that in our opinion it is fully adequate, in scope and quality, as a thesis for the degree of Master of Science.

_____

Assist. Prof. Dr. Alptekin Temizel

Supervisor

Examining Committee Members

Prof. Dr. Yasemin Yardımcı	(METU, II)	_____
Assist. Prof. Dr. Alptekin Temizel	(METU, II)	_____
Assist. Prof. Dr. Erhan Eren	(METU, II)	_____
Dr. Sevgi Özkan	(METU, II)	_____
Assist. Prof. Dr. İlkay Ulusoy	(METU, EE)	_____

I hereby declare that all information in this document has been obtained and presented in accordance with academic rules and ethical conduct. I also declare that, as required by these rules and conduct, I have fully cited and referenced all material and results that are not original to this work.

Name, Last name : Ali Sağlam

Signature : _____

ABSTRACT

ADAPTIVE CAMERA TAMPER DETECTION FOR VIDEO SURVEILLANCE

SAĞLAM, Ali
M.S., Department of Information Systems
Supervisor: Assist. Prof. Dr. Alptekin Temizel

June 2009, 54 pages

Criminals often resort to camera tampering to prevent capture of their actions. Many surveillance systems left unattended and videos surveillance system operators lose their concentration after a short period of time. Many important Real-time automated detection of video camera tampering cases is important for timely warning of the operators. Tampering can be defined as deliberate physical actions on a video surveillance camera and is generally done by obstructing the camera view by a foreign object, displacing the camera and changing the focus of the camera lens. In automated camera tamper detection systems, low false alarm rates are important as reliability of these systems is compromised by unnecessary alarms and consequently the operators start ignoring the warnings. We propose adaptive algorithms to detect and identify such cases with low false alarms rates in typical surveillance scenarios where there is significant activity in the scene. We also give brief information about the camera tampering detection algorithms in the literature. In this thesis we compare performance of the proposed algorithms to the algorithms in the literature by experimenting them with a set of test videos.

Keywords: video surveillance, camera tampering, camera sabotage, covered camera, defocused camera

ÖZ

VİDEO GÖZETLEME İÇİN UYARLANABİLİR KAMERA TAHRİFİ TESBİT ETME

SAĞLAM, Ali
Yüksek Lisans, Bilişim Sistemleri
Tez Yöneticisi: Yrd. Doç. Dr. Alptekin Temizel

Haziran 2009, 54 sayfa

Suçlular, suç işlerken görüntülerinin çekilmesini önlemek amacıyla kameraları tahrif etme yöntemine sıklıkla başvururlar. Bir çok video gözetleme sistemi gözetimsiz bırakılır ve kamera görüntülerini izleyen operatörler kısa bir sure sonra dikkatlerini kaybederler. Kamera tahrif edildiğinde kamera görüntülerini izleyen operatörlerin zamanında uyarılabilmesini sağlayan gerçek zamanlı ve otomatik tesbit önemlidir. Kamera tahrifi bir video kameraya yapılan kasıtlı fiziksel eylemler olarak tanımlanabilir ve genellikle kameranın görüşünü yabancı bir nesne ile engelleyerek, kameranın yerini değiştirerek, kamera lensinin odağını değiştirilerek yapılır. Kamera tahrifini otomatik belirleyen sistemlerde yanlış alarm oranının az olması önemlidir, çünkü yanlış alarmlar sistemin güvenilirliğini düşürür ve bunun neticesinde kamera görüntülerini izleyen operator sistemin uyarılarını göz ardı etmeye başlar. Bu tezde içerisinde önemli ölçüde hareket olan tipik gözetleme senaryolarında kamera tahrifini ve kamera tahrifinin ne şekilde yapıldığını tesbit etmek için uyarlanabilir algoritmalar sunuyoruz. Ayrıca literatürdeki kamera tahrifini tesbit etmek için kullanılan algoritmalar hakkında özet bilgi veriyoruz. Bu tezde bir test videosu kümesi ile deneyler yaparak bizim sunduğumuz kamera tahrifini tesbit etme algoritmalarının performansını literatürdeki diğer algoritmalar ile karşılaştırıyoruz.

Anahtar Kelimeler: Video Gözetlemek, Kamera Tahrifi, Önü Kapatılmış Kamera, Odağı Bozulmuş Kamera, Yeri Değiştirilmiş Kamera

ACKNOWLEDGMENTS

I am deeply grateful to my supervisor Assist. Prof.Dr. Alptekin Temizel, who has helped me throughout my research, and encouraged me in my academic life. He always had time to discuss things and showed me the way when I felt lost in my research. It was a great opportunity to work with him.

I would like to thank my colleagues at TÜBİTAK-UEKAE/G222 Unit, for their support and insightful comments. My sincere thanks also goes to my friends, Kadir Soydal and Selçuk Türkel for their help in capturing the test videos.

I would also like to address my thanks to The Scientific and Technological Research Council of Turkey (TÜBİTAK) for its scholarship during initial stages of my MS study.

Finally, I would like to thank my family and Rahime Belen for supporting my educational goals. Without their love, help and encouragement, this thesis has not been completed.

TABLE OF CONTENTS

LIST OF TABLES

TABLE

LIST OF FIGURES

FIGURE

LIST OF ABBREVIATIONS

FFT	: Fast Fourier Transform
ZNCC	: Zero-Mean Normalized Cross Correlation
VSAM	: Video Surveillance And Monitoring
1D	: One Dimensional
2D	: Two Dimensional
3D	: Three Dimensional
OpenCV	: Open Computer Vision Library
OS	: Operating System

CHAPTER 1

INTRODUCTION

"At the front door, we unscrew light bulbs, adjust cameras, cover them with rubber gloves if they do not move. Spray paint would be effective also at taking care of cameras that do not move.[1]*"*

Surveillance system operators often watch high number of cameras simultaneously and these systems are left unattended at certain times which result in important events that require immediate actions to be taken are missed such as deliberate attempts to tamper with a camera. In the recent years, computer assisted algorithms which analyze the images from the cameras and warn the operator regarding such events is found to be useful. In such systems, low number of false alarms is necessary. The high number of false alarms results in alarms being ignored by the operator and renders the system ineffective. Hence, such systems are expected to have low false alarm rate while having high true alarm success rate. Also low computational complexity is required as high number of cameras needs to be observed simultaneously or the algorithms are run on a camera or embedded system with limited computational power.

On 17 May 2009, we read from the news reports, "*Mexican authorities are conducting a massive manhunt after more than 50 inmates were freed in one of the most daring prison escapes in the country's escalating drug wars.* [2]". A video was captured from a security camera when this escape occurred. In this video, the prisoners cover the security camera with an object to prevent from being seen which is seen in Figure 1. If there had been a system which warns the surveillance operator when one of the security cameras is tampered, the escape may have been prevented.

Camera tampering which is also often referred to as camera sabotage in the literature, can be defined as deliberate physical actions on a video surveillance camera which compromises the captured images.

[1] Notes of a law enforcement officer to give readers some insight into the mind and methods of potential attackers: http://www.survivalblog.com/2009/02/real_world_observations_on_fig.html
[2] 17 May 2009 news on http://www.independent.co.uk/news/world/americas/more-than-fifty-escape-in-mexican-jailbreak-1686709.html

In this thesis we cover the following tampering types:

Defocused Camera View: Focus setting of a camera is changed and this results in reduced visibility.
Moved Camera: Turning a camera to make it point to a different direction.
Covered Camera View: Camera view is covered with a foreign object.

(a) (b) (c)

Figure 1: (a): Security camera view at time t_0 where a person is preparing to cover the camera view (b): Security camera view at time t_1 where a person starts to cover the camera view (c): Security camera view at time t_2 where a person covers the camera view

There are only a few methods in the literature which are aimed to detect the above sabotages. In this thesis, new methods are proposed to detect the above sabotage types and these methods are compared with the methods in [1-3]. In [1], wavelet based methods are proposed to detect defocused camera view and covered camera view. However no method is proposed to detect camera displacement. The algorithms proposed in paper [1] are based on a background model which is used as a base image together with its wavelet transform. In [2], an edge background model is used to detect camera tampering. However large objects or crowd of people moving in front of the camera could change the image characteristics significantly and cause false alarms. In [3], the authors propose keeping a short term and a long term pool of recent images. With each new image, these pools are updated and three dissimilarity functions are calculated for all the images in these pools. This makes real-time operation difficult due to the high number of computations required. Also this method doesn't identify the type of tampering as any kind of dissimilarity between the short term pool and the long term pool is flagged as tampering.

In this thesis we aim to detect camera tampering with robust methods which finds camera tampering events in different environments and generates fewer number of false alarms. These algorithms use an adaptive background image which is compared with the incoming frames from the video camera and with a delayed background image. We also keep track of the moving areas of the image and use a block based operation to reduce false alarms. This adaptive method is robust to moving objects in front of the camera.

Block diagram of the system is given in Figure 2. The system is composed of a video camera which is located on a non-moving surface and a platform such as PC where the algorithms are run. The system is based on the principle that when camera tampering occurs, the most recent frames captured by the camera will be significantly different than the background image which stores older frame's information. When a new frame is captured by the camera, firstly the background image is updated. After updating the background image sabotage detection algorithms compare the background image to the newly captured image to find whether a camera tampering has occurred. If no sabotage is detected, the system works usual. However, if the system detects any kind of sabotage, an alarm is triggered to warn the surveillance system operator.

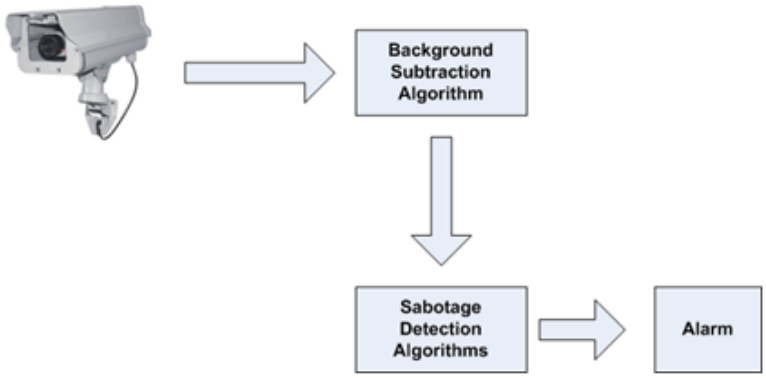

Figure 2: Block Diagram of the Camera Tampering Detection System

This thesis is composed of six chapters. Chapter 1 introduces the camera tampering types, and the approaches proposed in this thesis. In this chapter, we give introductory information about the system proposed in this thesis. Because background subtraction technique is used by the other techniques in the literature, we explain it before literature review in chapter 2. In this chapter, firstly the background subtraction methods in the literature are given. After that the background subtraction method that we use is explained and we discuss the rationale for choosing this particular technique. In chapter 3, the methods in the literature are given. In chapter 4, the algorithms to detect different camera tampering types are proposed. Detection of defocused camera view, detection of changed camera view and detection of covered camera view algorithms are separately explained. Following these, in chapter 5 the experimental results are given. Performance of the methods in the literature is compared to the methods which are proposed in this thesis and the results in various cases are discussed. In the last section conclusions and future work are summarized.

CHAPTER 2

BACKGROUND SUBTRACTION

2.1 Overview

Background subtraction is a widely used approach for segmenting out objects in the scene. We use this technique to detect the stationary parts of the video. As camera tampering makes newly captured frames significantly different than the older frames, we use estimated background images for camera tamper detection by comparing them to newly captured frames. There are several methods for performing background subtraction in the literature [4]. In this chapter we give information about these techniques. After that the background subtraction method used in the thesis is explained.

2.2 Background Subtraction Methods in the Literature

Background subtraction is used for segmenting out moving objects in a scene and finding the non changing parts of a scene. There are several methods to perform background subtraction in the literature. All these methods aim to estimate background view from a sequence of frames. These methods face many challenges to make good estimation of background model [5]**.** Illumination change is one of these challenges. Background subtraction methods must be robust against changes in illumination to give good results. Other challenges are non-stationary objects such as swinging leaves, rain, snow, shadow and speed of the background subtraction method.

In [4]**,** the author examines different background subtraction methods according to their speed, memory requirements and accuracy. These methods are:

- Running Gaussian average
- Temporal median filter
- Mixture of Gaussians
- Kernel density estimation (KDE)

- Sequential KD approximation
- Cooccurence of image variations
- Eigenbackgrounds

Running Gaussian average: This method is a pixel based background subtraction method. In this method, Gaussian probability density function is used for estimating background image's pixel values. The background model at each pixel location is based on the pixel's recent history [4]**.** The method is proposed in [6] and at each t frame, the I_t pixels value classified as non-stationary parts of the video if the inequality below is satisfied:

$$|I_t - \mu_t| > k\sigma_t \tag{2.1}$$

where k is a constant which can be used to change sensitivity. μ_t and σ_t are the two parameters of Gaussian probability density function. These values are calculated as:

$$\begin{aligned} \mu_t &= \alpha I_t + (1-\alpha)\,\mu_{t-1} \\ \sigma_t^2 &= \alpha(I_t - \mu_t)^2 + (1-\alpha)\sigma_{t-1}^2 \end{aligned} \tag{2.2}$$

where I_t is the current value of the pixel and μ_{t-1} is the previous average value. α is update parameter and used to change the stability of background model.

This method works fast and requires low memory. As the model is explained for intensity images like in [6], its extensions can be made for color images [4].

Temporal median filter: In this method the previous N frames of video are buffered, and the background is calculated as the median of buffered frames [7]. In his paper [4], Piccardi describes this method as "*The main disadvantage of a median-based approach is that its computation requires a buffer with the recent pixel values. Moreover, the median filter does not accommodate for a rigorous statistical description and does not provide a deviation measure for adapting the subtraction threshold.*"

Mixture of Gaussians: This method can handle multi model background distributions [5]. This technique is proposed in [8] and it provides a description both background and foreground. In [8] the probability of observing a certain pixel value, x, at time t is described by means of a mixture of K Gaussian distributions:

$$P(x_t) = \sum_{i=1}^{K} \omega_{i,t} * \alpha I_t + \eta(x_t, \mu_{i,t}, \sum_{i,t})$$
$$\eta(x_t, \mu, \sum) = \frac{1}{(2\pi)^{n/2}|\sum|^{1/2}} e^{-\frac{1}{2}(x_t-\mu_t)^T \sum^{-1}(x_t-\mu_t)} \quad (2.3)$$

where $\omega_{i,t}$ is an estimate of weight of the i^{th} Gaussian in the mixture at time t, $\sum_{i,t}$ is the covariance matrix of the i^{th} Gaussian in the mixture at time t, and where η is a Gaussian probability density function.

In this method, to discriminate background distributions from foreground distributions other properties of the distributions are used. In [4], it is given as "*first, all the distributions are ranked based on the ratio between their peak amplitude, ω_i, and standard deviation,σ_i. The assumption is that the higher and more compact the distribution, the more is likely to belong to the background. Then, the first B distributions in ranking order satisfying:*

$$\sum_{i=1}^{B} \omega_i > T \quad (2.4)$$

with T an assigned threshold, are accepted as background."

With this method, background subtraction can be done without keeping a large buffer of video frames. The accuracy of this model is higher when multi valued background is needed. When the objects in the background is not permanent like the scene consist of swinging leaves, rain, snow or sea waves, the performance of this method is better than the other two methods explained above [4].

Kernel Density Estimation: With this method the background probability density function is given by the histogram of the *n* most recent pixel values and each frame is smoothed with a Gaussian kernel [4]. Elgammal *et al.* in [9] proposed non-parametric method and in this method the background probability density function is given as sum of Gaussian kernels. The probability of observing a certain pixel value, *x*, at time *t* is described as:

$$P(x_t) = \frac{1}{n}\sum_{i=1}^{n} \eta(x_t - x_i, \sum_t) \quad (2.5)$$

where η is a Gaussian probability density function and $\sum_t$ is the covariance matrix at time *t*. If $P(x_t)$ is greater than a threshold the pixel, *x*, is classified as background.

Kernel Density Estimation method is more complex that the background subtraction methods explained so far [4]. This method requires high memory and works slow. However, the accuracy of

this method is high [9].

Sequential Kernel Density Approximation: Because mean-shift vector techniques which can be used for background estimation has a very high computational cost, Sequential Kernel Density Approximation technique proposed as an alternative [4]. In [10], Han *et al.* proposed a method which uses the mean-shift vector for only an offline model initialization. They detect the initial set of Gaussian modes of the background probability density function in the offline model initialization process. In this method, heuristic procedures are used for adaptation, creation and merging the existing modes to provide real time background model update.

In [10], Sequential Kernel Density Approximation method is compared to Kernel Density Estimation method by using 500 frame test videos. They found that; Sequential Kernel Density Approximation method is faster and requires lower memory than Kernel Density Estimation method.

Cooccurrence of image variations: In [11] Seki *et al.* propose a method which is based on the idea that neighboring blocks of background model's pixels vary in a similar way over time. They define stationary backgrounds impractical because the background scenes are not stable especially in the outdoor scenes. According to their experience, the performance of stationary backgrounds are bad when illumination changes and motions in background objects such as swinging leaves, rain or snow.

The proposed method in [11] aims to improve detection sensitivity by dynamically narrowing the ranges of background image variations for each video frame. In this method block based processing is done. This method is defined in two phases. In the first phase, a certain number of samples used to compute first the average for all the blocks then the difference to find image variations. After that covariance matrix and eigenvector transformation is computed. Aim of the first phase is to learn background image pattern. In the second phase, image blocks are classified as background or foreground. Eigen image variations of image blocks are used to classify these blocks as background or foreground.
Cooccurance of image variations method is a complex and effective method. According to experimental results in [4], this method is slower and requires more memory than all the other methods explained. However, the accuracy of this method is reasonably high.

Eigenbackgrounds: Eigenbackground subtraction is a commonly used method for segmenting out stationary parts of a video [12]. In this method newly coming frames are compared to background model to find foreground of a video by using eigen-value decomposition.

In [4] this method is explained in two phases. The first phase is called learning phase and in this phase

a certain number of video frames are acquired and an average image is computed. After that the covariance matrix is calculated and the best eigenvectors are stored in a matrix. In the second phase which is called classification phase, foreground and background pixels are detected. When a new frame is acquired from the video, it is projected onto the eigenspace. This projected image then projected onto the image space. Finally, absolute values of the difference of these two projected images' pixel values are compared to a threshold. If the value is greater than the threshold, corresponding pixel is classified as foreground.

According the experiments in [4]**,** the accuracy of this method better than the other methods explained above. Its memory requirements are proportional to the number of recent images which are used to calculate average image. The cost of the method about speed is associated with the number of best eigenvectors stored in the matrix.

2.3 Background Subtraction Method of Video Surveillance And Monitoring (VSAM) System

Among various methods for subtraction of background in the literature, we based ours on the adaptive background subtraction method of *Video Surveillance And Monitoring (VSAM) System* [13] as it provides a simple, low computational cost alternative. Even though there are more sophisticated background subtraction methods in the literature, we chose this method as the lower computational cost is more important than accuracy for camera tampering detection applications.

Let $I_n(x,y)$ represent the intensity value at pixel position (x,y) in the n^{th} frame. Estimated background image is represented as B_{n+1} and value at the same pixel position, $B_{n+1}(x,y)$ is calculated as follows:

$$B_{n+1}(x,y) = \begin{cases} \alpha B_n(x,y) + (1-\alpha) I_n(x,y) & if\ (x,y)\ is\ not\ moving \\ B_n(x,y) & if\ (x,y)\ is\ moving \end{cases} \quad (2.6)$$

where $B_n(x,y)$ is the previous estimate of the background intensity value at pixel position (x,y) and α is a positive real number where $0 < \alpha < 1$. α is selected close to 1 and $B_0(x,y)$ is set to the first image frame $I_0(x,y)$. A pixel is said to be moving if the corresponding intensity values in I_n and I_{n-1} satisfy the following:

$$|I_n(x,y) - I_{n-1}(x,y)| > T_n(x,y) \quad (2.7)$$

where $T_n(x,y)$ is an adaptive threshold value for pixels positioned at (x,y). After each background update, all the threshold values corresponding to each pixel position is also updated as follows:

$$T_{n+1}(x,y) = \begin{cases} \alpha T_n(x,y) + (1-\alpha)(c|I_n(x,y) - B_n(x,y)|) & if\ (x,y)\ is\ not\ moving \\ T_n(x,y) & if\ (x,y) is\ moving \end{cases} \quad (2.8)$$

where c is a real number greater than one. In this study we set initial values of all threshold values to 128 over 255. To increase the sensitivity the parameter c is reduced.

In this method, each pixel is compared to its corresponding adaptive threshold value to find whether the pixel is moving or not. These adaptive threshold values are updated according to (2.8) after all background estimation process. If a pixel is found as moving, its corresponding threshold value doesn't change. If a pixel is marked as not moving, its related threshold value is changed in terms of absolute value of the difference between current frame and background image's pixel values. Adaptive threshold makes the pixels in the background image where there is a high activity more sensitive to the changes in the current image.

Figure 3 shows the results of background subtraction for a scenario. In this figure, each row shows a certain time and each column shows change in the images which are used in the background subtraction method over time. Figure 3(a) shows the observed images, Figure 3(b) shows the background model for the observed images, Figure 3(c) shows the adaptive threshold values according to each pixel of the observed images and Figure 3(d) shows the foreground images.

In the first horizontal group of the figure two people are in the scene and they are moving at time t_0. As seen from the foreground image, these moving people are classified as foreground. Third image at time t_0, shows the adaptive threshold values and in this image the pixels that the two people are passing are distinctive. The values of these pixels which can also be depicted as moving pixels are greater than the other values in the adaptive threshold image. In our implementation of this background subtraction method, initial values of adaptive threshold values are set to 128. The adaptive threshold values of moving pixels are not changed according to (2.8) while the adaptive threshold values which are not moving are changed. In this case because the differences between the non moving pixels of I_n and B_n are not high, their corresponding adaptive threshold values are decreased. As seen from the adaptive threshold image, the values of non moving pixels are less than the values of moving pixels. In this background subtraction method, background model is slowly updated. When a new object enters the scene, it takes a certain time to the object to become hardly visible in the background. Similarly, when an existing object leaves the scene, it takes a certain time to the object to be removed from the background. In the first horizontal group, some scarcely visible objects are seen in the background image. The people who are passing through the scene are scarcely visible in the background image. Because they are not stationary, they don't become hardly visible in the background image. On the contrary, the scarcely visible objects in the background image will be invisible after a short period of time.

In the second horizontal group of Figure 3 there are no moving objects in the scene at time t_1. The people who were passing through have left the scene. Because the input image consists of stationary objects, the foreground image is seen as totally black. In the background image of this group the scarcely visible objects which are seen in the previous background image become invisible. Adaptive threshold image of this group is also different from the previous one. All the pixels of the input image are classified as not moving and this causes the adaptive threshold values to change.

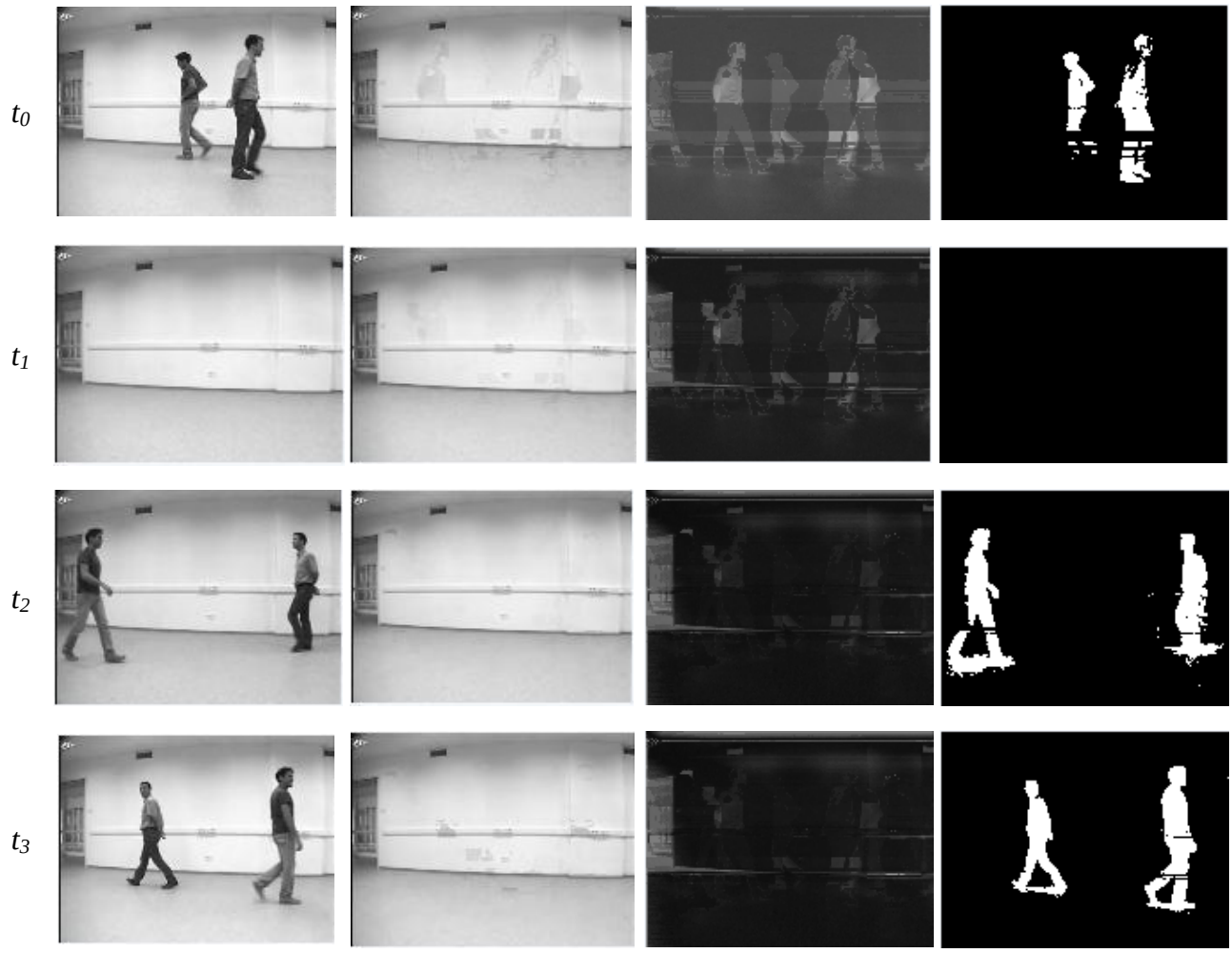

Figure 3: Background Subtraction Method of VSAM system. In this figure, horizontal groups show the relation between input, background, adaptive threshold and foreground. This scenario is running from top to down.

In the third horizontal group, the two people again enter the scene at time t_2. In the foreground image, the pixel values where the two people are standing are specified with white values. Because threshold values are adapted over time, this time the pixels that the people are passing are not seen in the

background image. In the first horizontal group, the pixels can be seen scarcely visible in the background image. Over time adaptive threshold values changed to enhance background estimation.

In the last horizontal group of Figure 3, the two people are seen in the scene and this causes the corresponding pixel values to have white values in the foreground image at time t_3. Background image of this group consists of stationary parts of the video.

When an object enters or leaves the scene, it takes some time to the background model to become free from moving objects. If the background subtraction method detects a new object in the scene which is not exist in the previous scene, and the related pixels are not moving, the objects start to become a part of background model. In a similar way, when an object leaves the scene and the related pixels are classified as non-moving, the background model starts to be updated to make the object invisible. In Figure 4 a new object enters the scene and the background model updates over time. In the end, the object becomes hardly visible in the background image.

(a) (b) (c)

Figure 4: (a): Background image at time t_0 (b): Background image at time t_1 where a new object has entered the scene (c): Background image at time t_2 where the object is hardly visible

CHAPTER 3

LITERATURE REVIEW

3.1 Overview

In this chapter we review the existing approaches for camera tamper detection in the literature. There are methods to detect tampering of recorded images. For example, in [14] a watermarking technique is proposed for tamper detection in digital images. This method divides images into blocks and by comparing correlation values from different blocks of the images it enables us to distinguish malicious changes. Another method proposed by Roberts in [15] and this method aims to authenticate images captured by a security camera and localise tampered areas.While these methods bring new contributions, they are not directly related to our problem. In this thesis we aim to create some methods which monitors live video and detects defocused camera view, moved camera and covered camera view.

There are many researches in computer vision which can be used to detect defocused camera view, moved camera and covered camera view. However these methods are not directly concentrated on camera tamper detection problem. In order to detect defocused camera view there are many researches which may be employed. For example, Lim *et al.* in [16] proposed a method which aims to detect out-of-focus photographs. They describe an algorithm that automatically determines if the captured photograph is out-of-focus through image analysis. This method is specialized for digital photograph machines and may not convenient in our case. This and similar methods are work on a single image. In our case, there may be some transient conditions that single frame of a video may be out-of-focus not implying camera tampering.

There are also many techniques which might be employed to detect covered camera view. For

example, in [17] a technique is proposed in order to detect gradual transitions in video sequences and automatically identifying its type. This technique works fine when smooth transitions occur. However, camera tampering is a rapid action that physically affects camera view. In [18] a method is proposed to detect scene change which is also depicted as shot change. The technique is based on the tracking boundary points in the edges, which is resistant to object motions and works well under gradual transition. Because there are essential differences between camera tampering detection and shot detection, this technique is not adequate for detecting covered camera view. Shot detection is used to split up a video into basic temporal units which are called shots, while detection of covered camera view is concerning of camera tampering.

In [19] a factorization method is proposed in order to estimate camera motion from stream of images. It gives information about motion of the camera. In [20] another method is proposed to detect camera motion. This approach minimizes both image error (i.e. noise) and the epipolar error (geometric problem which occurs when projecting a 3D point onto the 2D images) to get optimal motion estimation. Both of these methods are one of the studies in the camera motion estimation area. However, these and similar techniques are not convenient for estimating camera motion where a person moves it to point in a different direction. In our problem estimation of the motion of the camera is not as important as simply recognizing that camera motion has occurred.

There are only a few methods in the literature which are directly aimed to detect camera tampering. These methods all take a live video as input, and detect one or more sabotage types explained above. In [1], wavelet based methods are proposed to detect defocused camera view and covered camera view. However no method is proposed to detect camera movement. In [2], the methods for detecting camera tampering are based on an edge based background model. This background model is not robust against large objects or crowd of people moving in front of the camera and this result in false alarm detection. In [3], short term and long term pools are used. When a new frame acquired from video, these two pools are updated and three dissimilarity functions are calculated for all images in these pools. Computational complexity of this method is very high and it doesn't identify the sabotage type as defocused camera view, moved camera view and covered camera view. In [21], some methods are proposed for surveillance systems inside a moving platform such as vehicle. Because our problem is concerning the camera tampering where the camera is located on a steady place, the methods in this research are not investigated in detail.

In the rest of this chapter we give more information about the techniques proposed in [1-3]. Their established strengths and weakness are explained in more detail.

3.2 Camera Tamper Detection Using Wavelet Analysis for Video Surveillance

In this method, two algorithms are proposed to detect covered camera view and defocused camera view [1]. These two algorithms are based on a background model which is proposed in [13]. The background subtraction method is extended in this research to make it work in wavelet domain. The authors estimate the background scene from the wavelet coefficients. Foreground objects and their wavelet transform changes in time. The equations given in [13] which are used to estimate background view and adaptive threshold values are modified as follows:

$$\mathrm{W}^{\mathrm{j}}B_{n+1}(k,l) = \begin{cases} \alpha \mathrm{W}^{\mathrm{j}}B_n(k,l) + (1-\alpha)\mathrm{W}^{\mathrm{j}}I_n(k,l) & if\ \mathrm{W}^{\mathrm{j}}\mathrm{I}_{\mathrm{n}}(x,y)\ is\ not\ moving \\ \mathrm{W}^{\mathrm{j}}B_n(k,l) & if\ \mathrm{W}^{\mathrm{j}}\mathrm{I}_{\mathrm{n}}(x,y)\ is\ moving \end{cases} \tag{3.1}$$

$$\mathrm{W}^{\mathrm{j}}T_{n+1}(k,l) = \begin{cases} \alpha \mathrm{W}^{\mathrm{j}}T_n(k,l) + (1-\alpha)\left(c\left|\mathrm{W}^{\mathrm{j}}I_n(k,l) - \mathrm{W}^{\mathrm{j}}B_n(k,l)\right|\right) \\ \qquad\qquad , if\ \mathrm{W}^{\mathrm{j}}\mathrm{I}_{\mathrm{n}}(x,y)\ is\ not\ moving \\ \mathrm{W}^{\mathrm{j}}T_n(x,y) \qquad , if\ \mathrm{W}^{\mathrm{j}}\mathrm{I}_{\mathrm{n}}(x,y) is\ moving \end{cases} \tag{3.2}$$

where $W^jB_n(k,l)$ shows the coefficient value of the wavelet image for pixel positioned at k,l.

To detect covered camera view, this method uses histogram values of the current frame and the background frame. Maximum values of the histogram values are compared to check if the current value has a higher peak than the background value. After that, histogram of absolute difference image is checked to see the amount of values near the black end. These comparisons are done in low-low wavelet band. This selection increases the robustness of the algorithm, because small changes are discarded by the low-pass filter of wavelet transform.

When a camera view is defocused, small scale detail of the video disappears. In this method wavelet low-high, high-low and high-high sub-bands are used for calculating the high frequency values of current image and background image. Edges of the images are available in these sub-bands. High frequency data of current image and background image is calculated in the following equations:

$$\begin{aligned} \mathrm{E}_{\mathrm{HF}}(I_n) &= \sum_{k,l}|W_{LH}I_n| + \sum_{k,l}|W_{HL}I_n| + \sum_{k,l}|W_{HH}I_n| \\ \mathrm{E}_{\mathrm{HF}}(B_n) &= \sum_{k,l}|W_{LH}B_n| + \sum_{k,l}|W_{HL}B_n| + \sum_{k,l}|W_{HH}B_n| \end{aligned} \tag{3.3}$$

where $W_{LH}I_{n,}$ $W_{HL}I_n$ and $W_{HH}I_n$ are the horizontal, vertical and diagonal sub-bands of single stage wavelet transform of $\mathrm{I_n}$ respectively. High frequency value of current image and the background image are compared with some tolerance to detect whether the camera view is defocused or not. If high

frequency value of current image is smaller than the high frequency value of background image, the camera view detected as tampered.

In this camera tamper detection method there are some techniques which aim to reduce false alarm detection rate. Persistency check is one of the measures against false alarms. This function checks if the tampering cases occur in different consecutive time instants before triggering an alarm. Edge correspondence check is another method for reducing false alarm rate. In this function camera view is checked to confirm that camera still monitoring the same scene. If it is not, the results of covered camera view and defocused camera view algorithms are discarded. Last measure is low light conditions. If the level of light is less than a threshold, no calculation is done to find camera tampering.

3.3 Automatic Control of Video Surveillance Camera Sabotage

In this method [2], three algorithms are proposed to detect covered camera view, moved camera and defocused camera view. These algorithms are based on an edge based background model. The main concept is the comparison between the new frames with the older frames called the background model.

The background model which is used in this camera tamper detection technique includes only the information at the edges of the stationary objects belonging to the background. The background image contains information on the edges of the current image. To ensure that an edge belongs to the background image, the following calculation is done for *M* consecutive frames.

$$B_n = \sum_{i=nM}^{(n+1)M-1} D_i \tag{3.4}$$

where D_i is the edge matrix computed for frame i. The pixels in D_i take value 1 if it belongs to an edge and 0 otherwise. To allow the system for slow changes of the background, the matrix B is computed for each M new frames, and the background image is updated according to:

$$P_n = \alpha P_{n-1} + (1-\alpha) B_n \tag{3.5}$$

where α is a parameter between 0 and 1. If it is closer to 1 the background updates slowly. Only the pixels which have been computed as edges for an enough number of times (the authors in [2] set it $P_n \geq M/2$) are considered to belong to the background model.

The entropy of the pixels belonging to the background model is computed to detect whether the camera view is covered or not. When camera view is covered partially or totally by an object, the corresponding pixels in the background image turn to zero. In this situation, the entropy of the background image decreases. Entropy is calculated as follows:

$$E = -\sum_{k} P_k \, ln(P_k) \tag{3.6}$$

where P_k is the probability of appearance of the gray level k in the image. Because *ln(0)* is equals to infinity entropy calculation isn't done when P_k equals to zero. Depending on the background model this calculation is done after each M consecutive frame arrives. In this method camera view is said to be covered when the current entropy is smaller than a threshold. This method may be extended for partially covered camera view cases. To enable the system to detect partially covered camera view, the image is divided into blocks of equal size and entropy calculation is done for each block. In this extended method, sabotage is detected when the current entropy for at least one of these blocks are smaller than a threshold.

Defocused camera view results in degradation of the edges. In this camera tamper detection method, the authors simply compare the number of edges in the background image and the current image. When a camera view is defocused, the number of edges in current image will be significantly lower than the number of edges in the background image.

In this research a block matching algorithm is used to detect whether camera view is moved or not. Zero-Mean Normalized Cross Correlation (ZNCC) is calculated from the current frame and the previous frame to match them. To speed up the calculations, only the pixels of the background model are taken into account. This method tries to match the same edges of current frame and previous frame and by this way it finds the amount of shift between two frames. If the shift is greater than a threshold, camera view is said to be moved. Zero-Mean Normalized Cross Correlation is calculated as follows:

$$ZNCC = \frac{\sum_{x,y}\left(I_{i-1}(x,y) - \mu_{I_{i-1}}\right)\left(I_i(x+m, y+n) - \mu_{I_i}\right)}{\sigma I_{i-1} \sigma I_i} \tag{3.7}$$

where I_i denotes current frame, I_{i-1} denotes the previous frame, μ is the average value, σ is the standard deviation, m is the horizontal axes and n is the vertical axes. The calculation is started from m and n equals to zero and incremented up to the point where the ZNCC result is good enough. To speed up algorithm ZNCC calculation isn't done if there is no edge on the *(x,y)* and *(x+m,y+n)* pixels of the background image. If there is no displacement, the result of ZNCC equals to multiplication of width and height of the image. If the result is smaller than a given threshold, it is interpreted as an error and simply discarded. Displacements are tolerated up to 5 pixels. If it is greater than 5, an alarm is triggered by this algorithm.

3.3 Real-Time Detection of Camera Tampering

The method described in [3], is based on the principle that when camera tampering occurs, the most recent frames of video will be significantly different than the older frames. In this method, the frames

which are acquired from video are stored in two different buffers. These buffers are called short term pool and long term pool. Short term pool keeps newly coming frames and the size of this pool is 3-15 images depending on the setting chosen by the user. Long term pool keeps older frames and it stores higher number of frames. When a frame is acquired from the video, it is stored in the short term pool. If the number of frames in the short term pool is more than the allowed, the oldest frame is evicted from the short term pool and inserted into the long term pool. Frames which are evicted from long term pool are no longer stored. This structure may be thought as an alternative to the background model in other camera tamper detection methods.

Each time a new frame is pushed into the short term pool, the short term pool and long term pool are compared in order to determine if camera tampering has occurred. Every frame in short term pool is compared to every frame in long term pool. Three dissimilarity functions are calculated for all these comparisons. Medians of these three measurements are taken and compared to their corresponding thresholds. The thresholds are tuned for optimal performance according to training videos. If any of the thresholds are exceeded, the decision is made that camera tampering has occurred. However, this method doesn't identify the type of tampering and as there are too many calculations in this approach, it makes real-time operation difficult.

One of the image dissimilarity functions is histogram chromaticity difference. For each image a normalized RGB histogram is calculated. In these histogram two axes shows the normalized red and green components of each pixel. Blue component in this representation is uniquely determined by the other two and ignored. The bin assignment for the 2D histogram is calculated as follows:

$$\begin{aligned} Bin_R &= R_i NumBins_R/(R_i + G_i + B_i) \\ Bin_G &= G_i NumBins_G/(R_i + G_i + B_i) \end{aligned} \tag{3.8}$$

where R_i, G_i and B_i are the red, green and blue components of pixel *i*. The value of Bin_R and Bin_G in the 2D histogram is incremented after this calculation. For example, the 2D histogram consists of 64 bins and the results for Bin_R and Bin_G are calculated as the following:

$Bin_R = 25$

$Bin_G = 78$

The value of bin expressed in Figure 5 incremented by one. In this figure 8x8 bins exist and the results of Bin_R and Bin_G are normalized according to the number of bins.

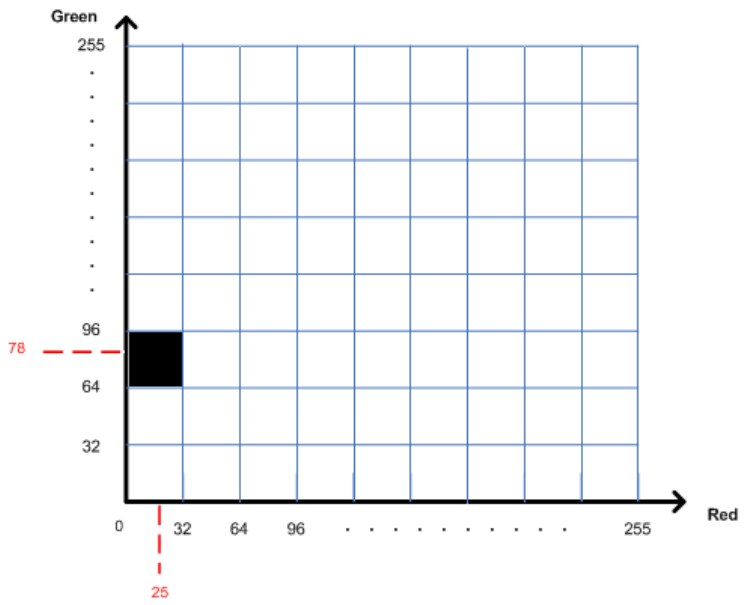

Figure 5: 2D Histogram Bin Assignment

To calculate histogram chromaticity difference, the sum of absolute value differences of the two histograms is computed. This difference is given as:

$$Difference_{1,2} = \sum_{i,j} |H_1(i,j) - H_2(i,j)| \tag{3.9}$$

When a new frame pushed into the short term pool, the difference is calculated for all the frames in the short term and long term pools. After that the median value is taken and compared to a threshold value. If it exceeds the threshold value, the condition is evaluated as true which means that camera tampering has occurred.

Histogram L1R difference is another dissimilarity function which is used to detect camera tampering. In this function, a 2D histogram is used again. However the axes of this 2D histogram are different than the previous one. The axes of this histogram are the L1-norm and range of the red, green and blue components of the pixel. The bin assignments are calculated as follows:

$$\begin{aligned} Bin_{L1} &= (R_i + G_i + B_i) NumBins_{L1}/3 \\ Bin_G &= \big(\max(R_i, G_i, B_i) - \min(R_i, G_i, B_i)\big) NumBins_R \end{aligned} \tag{3.10}$$

where R is the range and $L1$ is the L1-norm. In this 2D histogram total number of bins may be different than the previous one. L1-norm value of a pixel is proportional to its intensity and the range is proportional to its saturation. The dissimilarity between two images is calculated again by summing the absolute values of differences between the two histograms. Similarly, this measurement is done when a new frame is pushed into the short term pool. Median value is compared to a threshold and if it is greater than a threshold, camera view is said to be tampered.

The last dissimilarity function proposed in this method is histogram gradient direction difference. In this function each image is firstly convolved with the 3x3 Sobel kernels. After that, these images are used to estimate gradient direction. In this dissimilarity function 1D histogram is used. The bin assignments in this 1D histogram are done in a similar way. The bin assignment for pixel *(i,j)* is calculated as:

$$Bin_{GradDir} = 1/\pi(Dir(i,j) + \pi/2)NumBins_{GradDir} \quad (3.11)$$

where $Dir_{i,j}$ is the gradient direction at pixel location *(i,j)*. Gradient direction is thought as in the range [-π, π]. Sum of absolute values of differences between two histograms are used as dissimilarity. Each frame in short term pool and long term pool is compared with this image dissimilarity. The median values are compared to a threshold to find whether the camera view is tampered or not.

CHAPTER 4

ADAPTIVE CAMERA TAMPER DETECTION ALGORITHMS

4.1 Overview

In this chapter, we will explain the proposed algorithms which are used to detect defocused camera view, moved camera and covered camera view. Firstly, we explain the detection of defocused camera view method. In this method we use high frequency data of current and background frames to find whether the camera view is defocused or not. After that we investigate the cases where the amount of high frequency changes significantly. For these cases an extension of this method is proposed. In this extended method, regularly changing parts of the images are ignored to reduce false alarm rate. Secondly, we explain the detection of moved camera method. In this method, we use a delayed background image and this image is compared with the background image to find if the camera is moved to point in a different direction. Lastly, we give information about the detection of covered camera view method. In the first step of this method histograms of the current and background images are compared to detect whether camera view is covered or not. In the second step, histogram of absolute difference image $|I_n\text{-}B_n|$ is checked to see if most of the values are located near the black end.

4.2 Detection of Defocused Camera View

Defocusing the lens of a camera or reduced visibility due to atmospheric conditions such as fog results in degradation of edges in the captured image. In such a case, the high frequency data of the current image I_n will be lower than the high frequency data of the background image B_n. In the proposed algorithm, high frequency data in I_n and B_n are compared using Fast Fourier Transform (FFT). In Figure 6 two frames of a video and their corresponding magnitude images which are obtained after taking FFT are given. In the magnitude images, high frequency values are around the origin. In the first horizontal group, camera view isn‘t defocused and the image has strong edges resulting in high frequency data in the magnitude image. In the second horizontal group, camera view is defocused

which results in loss of high frequency data in the corresponding magnitude image. Because small scale detail of the video disappears when the camera view is defocused, some of the low frequency values are also lost from the images.

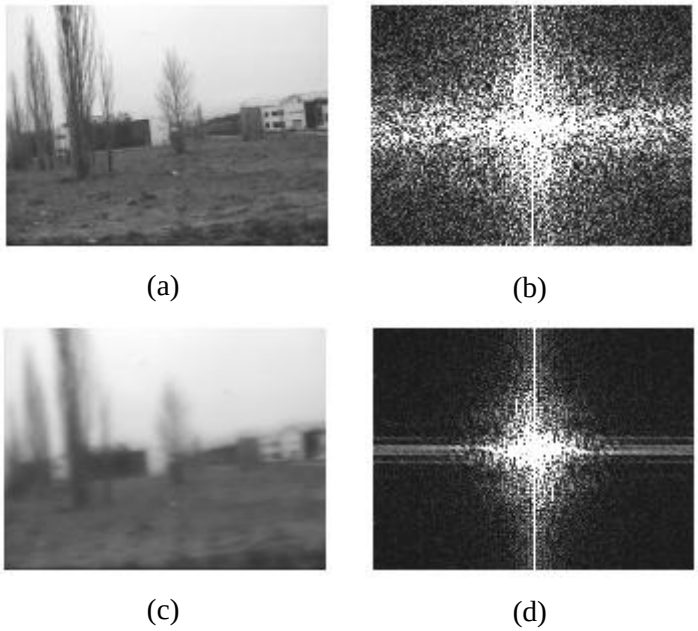

(a) (b)

(c) (d)

Figure 6: (a): Normal (non-defocused) camera view, (b): magnitude image of the non-defocused camera view after taking FFT (c): defocused camera view, (d): magnitude image of the defocused camera view after taking FFT

After taking Fourier Transform of the images, a Gaussian windowing function is used to discriminate the higher frequency values from lower frequencies. Let $E_{HF}(I_n)$ be the sum of high frequency values of I_n which is calculated as follows:

$$E_{HF}(I_n) = \sum_{x,y} G(x,y).F\{I_n(x,y)\} \tag{4.1}$$

where $G(.)$ is the Gaussian windowing function which will be used to eliminate low frequency values and $F\{.\}$ indicates Discrete Fourier Transform. $G(.)$ is obtained by taking Discrete Fourier Transform of a Gaussian window of which size is equal to I_n.

Similarly, sum of high frequency values of B_n will be called $E_{HF}(B_n)$ and calculated as follows:

$$\mathrm{E_{HF}}(B_n) = \sum_{x,y} G(x,y).F\{B_n(x,y)\} \tag{4.2}$$

Figure 7 shows a wireframe representation of a Gaussian windowing image which is used to discriminate high frequency values from low frequencies. The size of this window is equal to the size of the magnitude image and all the pixels in the magnitude image are multiplied with the

corresponding pixels of the Gaussian windowing image. By this way, the highest frequency which is found on the origin of the magnitude image is multiplied with the highest coefficient; the lower frequencies are multiplied with lower coefficients.

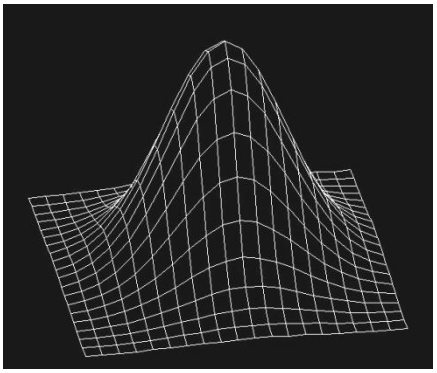

Figure 7: Gaussian Window

After these two functions, all pixels of I_n and B_n are summed to find $E_{HF}(I_n)$ and $E_{HF}(B_n)$. A camera lens is said to be defocused if;

$$E_{HF}(I_n) < \mathrm{T}h_1 E_{HF}(B_n) \tag{4.3}$$

where $0<Th_1<1$ is a threshold, the detection sensitivity increases when Th_1 is closer to 1. In this method, Th_1 is updated by taking into account the level of detail in the background image before applying equation (4.3). If the camera watches a scene with large uniform areas, the amount of high frequency data is expected to be low. Hence, defocusing camera view doesn't change the amount of high frequency data too much. In this situation, the threshold is set to a number which is closer to 1 to increase the sensitivity. If the camera watches a scene which contains large amount of high frequency data, the method is expected to be more sensitive. In this case, some events may be misinterpreted as defocused. To reduce the number of false alarms, the threshold is set to a number which is closer to 0 to decrease the sensitivity.

The threshold is updated according to the following equation:

$$Th_1 = \begin{cases} 1 - L_{Bound} & ,if\ 1 - (E_{HF}(B_n)/Max_{HF}) \leq L_{Bound} \\ 1 - \dfrac{E_{HF}(B_n)}{Max_{HF}} & ,if\ \ U_{Bound} \geq 1 - (E_{HF}(B_n)/Max_{HF}) \geq L_{Bound} \\ 1 - U_{Bound} & ,if\ 1 - (E_{HF}(B_n)/Max_{HF}) \geq U_{Bound} \end{cases} \tag{4.4}$$

where $E_{HF}(B_n)$ is the high frequency data of B_n and calculated in the same way as equation (4.2). We use B_n to find the level of detail in the scene because B_n is more stable than I_n. Max_{HF} is an experimentally determined value which depicts the maximum number that $E_{HF}(B_n)$ can take. L_{Bound} and U_{Bound} indicate lower and upper bounds of the Th_1. In our implementation, we set L_{Bound} to 0.4 and U_{Bound} to 0.8. We experimentally determined that, the probability of false alarms and missed events is

higher when the threshold is smaller than L_{Bound} and greater than U_{Bound}. Because of that, we don't allow the threshold to exceed these bounds.

In Figure 8, two images and their magnitudes are given. In Figure 8 (a) camera watches a scene which contains less high frequency data and in Figure 8 (c), the same scene seen as defocused. As seen from the magnitude images, the amount of high frequency data in defocused and non-defocused images are not so different. In this case, we reduced the number of missed events by updating the threshold. The magnitude images shown in this figure are filtered with a Gaussian windowing function.

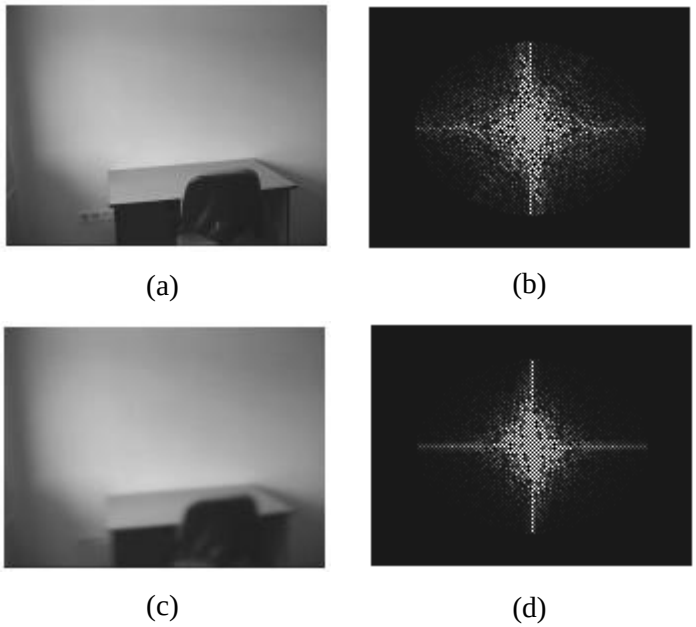

Figure 8: (a): non-defocused camera view with large uniform areas, (b): magnitude image of the image (a) filtered with a Gaussian window (c): defocused camera view with large uniform areas, (d): filtered magnitude image of the (c) filtered with a Gaussian window

In Figure 9, two camera views which are captured from the same scene and their magnitudes are given. In Figure 9 (a), the amount of high frequency data is high. If this view is defocused as seen in Figure 9 (c), the change of high frequency data in the magnitude image will be reasonably high. In this situation, we reduced the number of missed events by setting the threshold to a number which is closer to 0. The magnitude images shown in this figure are filtered with a Gaussian windowing function.

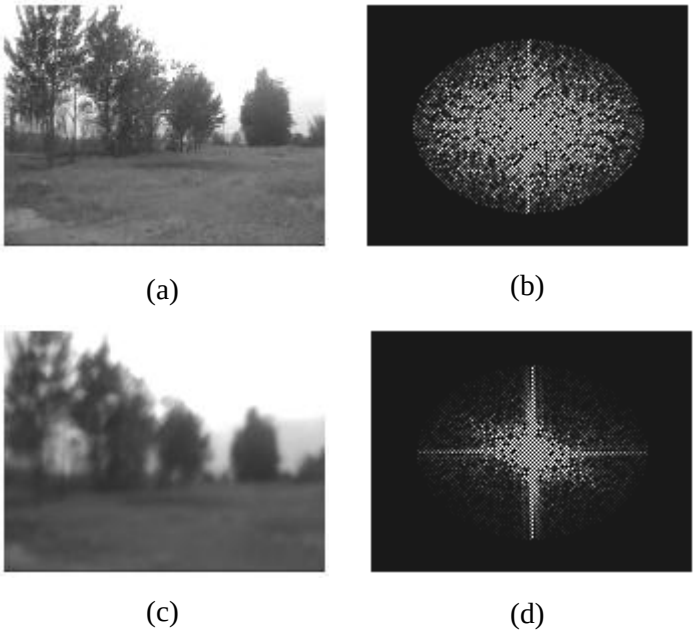

(a) (b)

(c) (d)

Figure 9: (a): non-defocused camera view with large high frequency data, (b): magnitude image of the image (a) filtered with a Gaussian window (c): defocused camera view with large high frequency data, (d): filtered magnitude image of the (c) filtered with a Gaussian window

Even though this method is useful for detecting the reduced visibility, there are cases in typical surveillance scenarios where the amount of high frequency changes significantly which could potentially generate false alarms. When new objects enter to the scene or objects leave the scene, total amount of edges and hence the high frequency content in I_n changes. To handle such cases, the algorithm is modified to ignore regularly changing parts of the images. Changing pixels are found and marked using equation (4.5) and they are kept in moving state until they are observed to be non-moving for a while.

$$M_n(x,y) = \begin{cases} M_n(x,y) + \beta|I_n(x,y) - B_n(x,y)| \\ \quad ,if\ (x,y)\ is\ moving \\ \\ M_n(x,y) - \gamma|I_n(x,y) - B_n(x,y) + 1| \\ \quad ,if\ (x,y)\ is\ non\ moving \end{cases} \tag{4.5}$$

In this equation, M_n is the image which keeps track of the changing pixels related to n^{th} frame. Initial values of its pixels are set to 0. β and γ are constants and β is selected to be greater than γ to make a pixel gracefully non-moving when no motion is observed.

Figure 10 shows the change of high frequency values when new objects enter or leave the scene.

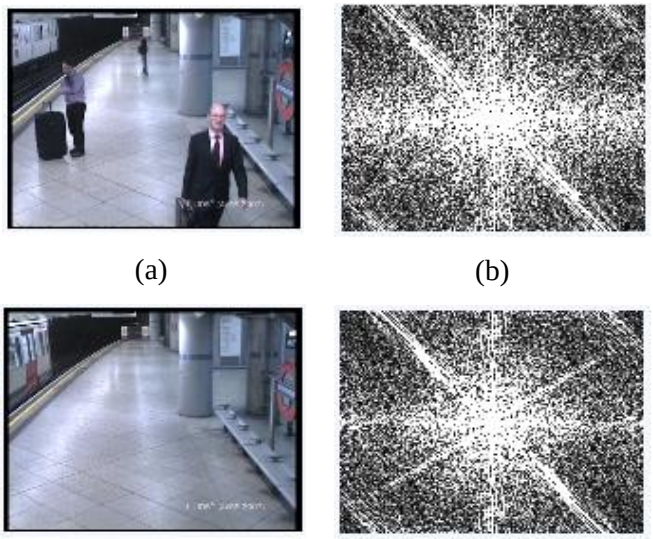

(a) (b)

(c) (d)

Figure 10: (a): An image which contains more high frequency component, (b): Magnitude of the image (a) after FFT, (c): An image which contains less high frequency values, (d): Magnitude of the image (b) after taking FFT.

After finding the changing pixels, I_n and B_n divided into 8x8 pixel blocks. Each block is checked for moving pixels, if the block contains any moving pixels, the pixels in this block are excluded from the equation calculating the high frequency content in both I_n and B_n. Figure 11 shows an example of exclusion of moving areas.

(a) (b)

Figure 11: (a): Image showing changing pixels, M_n where changing pixels are shown white (b): Corresponding image which shows the ignored blocks. Black rectangles show the ignored areas.

Amount of high frequency data in I_n and B_n are calculated using the following equations which excludes the moving blocks. A block is said to be moving if $M_n(x,y) \neq 0$ for any pixel in the block:

$$E_{HF}(I_n) = \sum_{i=0}^{k} \sum_{x,y} G(x,y).F\{I_n(x,y)\} \tag{4.6}$$

$$E_{HF}(B_n) = \sum_{i=0}^{k} \sum_{x,y} G(x,y).F\{B_n(x,y)\} \tag{4.7}$$

where k is the number of blocks not having any moving pixels. Once $E_{HF}(I_n)$ and $E_{HF}(B_n)$ are found, they are compared using the equation (4.3). Th_1 is updated in the same way to equation (4.4). The $E_{HF}(B_n)$ which is used to update Th_1 is calculated without block based processing.

4.3 Detection of Moved Camera

Turning a camera to make it point in a different direction is also a type of tampering. When a camera is moved to a different direction, the background image B_n starts to be updated to reflect the changed view. In the proposed algorithm we use another image which holds a delayed background image and represented as B_{n-k} where $k \epsilon Z^+$. B_{n-k} is compared with B_n to find if a camera is moved to point towards a different direction. A proportion value denoted with P is calculated by comparing each pixel on B_n to corresponding pixel on B_{n-k}.

$$P = \begin{cases} P+1 & ,if\ B_n(x,y) \neq B_{n-k}(x,y) \\ P & ,if\ B_n(x,y) = B_{n-k}(x,y) \end{cases} \tag{4.8}$$

Camera is said to be moved to different direction if $P>Th_2K$ where $0<Th_2<1$ is threshold value which increases sensitivity when it is closer to 0 and K is the total number of pixels.

Figure 12 shows the input, background and delayed background images when the camera is turned to a different direction. At time t_0, the camera hasn't been moved yet and as seen from the figure the three images have the same scene. When the camera is moved at time t_1, the background image starts updating, while the delayed background image doesn't change yet. The background image changes totally at time t_3 while the delayed background still reflects the earlier scene.

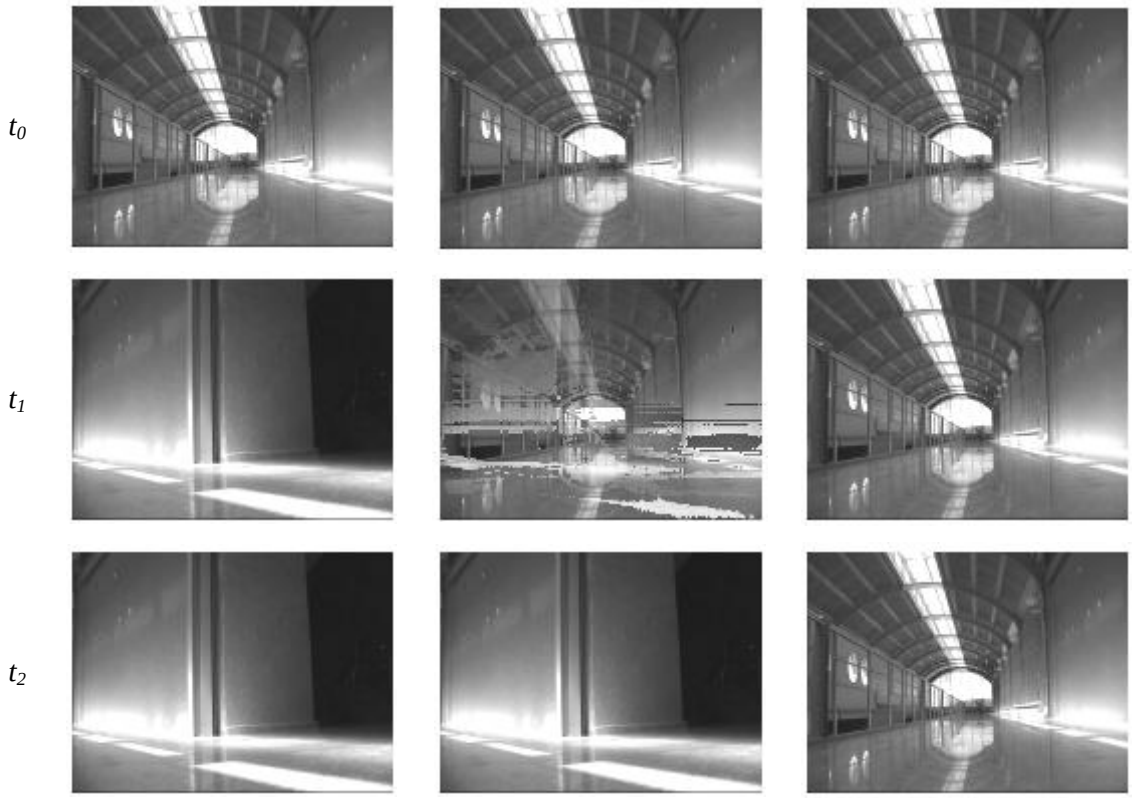

Figure 12: (a): Input image which is captured from the camera (b): Estimated background image B_n, which starts to be updated when camera is turned to different direction, (c): Delayed background image B_{n-k}.

Similar to the detection of defocused camera view method, the threshold Th_2 is updated adaptively in relation to the amount of high frequency component in the background image. If the view consists of large uniform areas and camera is turned in a different direction, the pixels in the new scene will not be so different from the previous scene. In this situation, by changing Th_2 sensitivity is increased to detect moved camera. In Figure 13 camera is firstly looking to an area with few detail. This view has large amount of uniform areas and when it is turned to different direction as in the figure, most pixels in the new scene have similar values with the previous scene. In this case, the proportion value calculated in (4.8) will not be high. To detect moved camera, the threshold value set to a number which is closer to 0. We update the threshold value Th_2 in relation to the amount of high frequency component in the background image to decrease number of missed events.

(a) (b)

Figure 13: (a): Camera view where there are large uniform areas (b): Turned view of (a) where most of the pixels have the similar values with the previous scene

4.4 Detection of Covered Camera View

When a camera view is covered with an object, histogram of I_n is expected to have higher values in a specific range in the histogram compared to the B_n. Because most of the scene is occupied by the covering object, a significant part of I_n is expected to have the color of the covering object or become darker. In Figure 14, current and background images and their corresponding 32-bin histograms are given when camera is covered by hand.

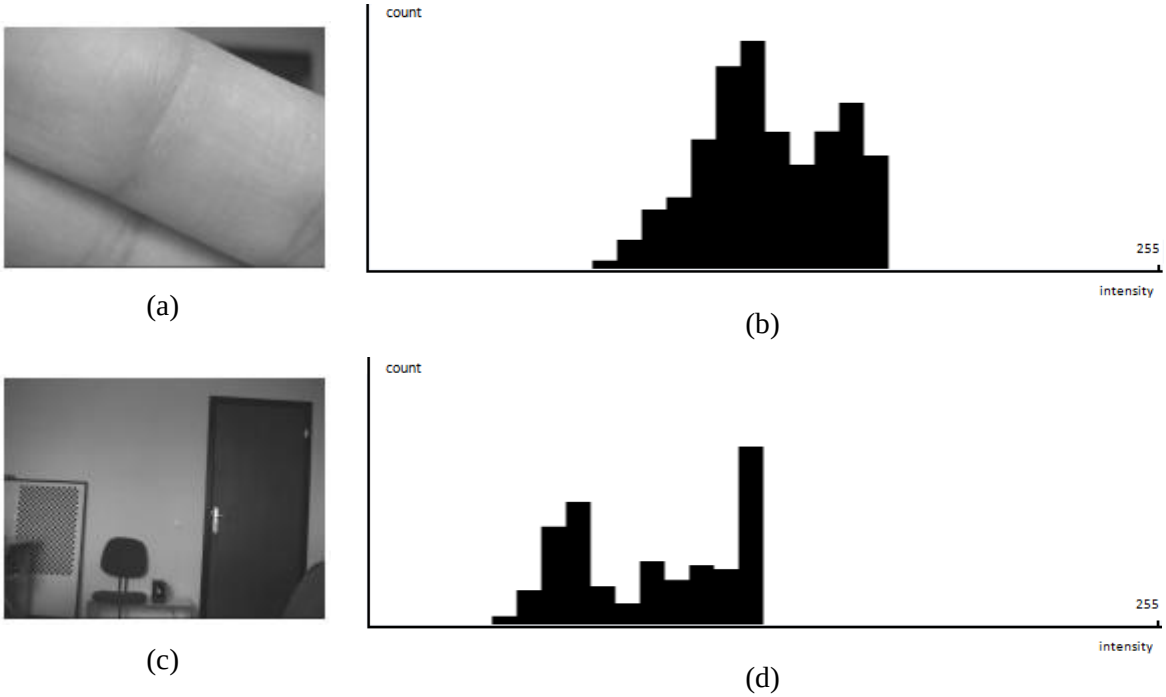

(a) (b)

(c) (d)

Figure 14: (a): I_n when camera covered (b): Histogram of the image I_n when camera covered (c): B_n when camera covered (d): Histogram of the image B_n when camera covered

In [1], an algorithm which is used to detect covered camera view is proposed. The algorithm calculates the histograms of I_n and B_n. In this algorithm there are two steps. If both of the steps are satisfied, camera view is said to be covered. In this study we modified the first step of this algorithm. Let *max(H(A))* represent the bin number of which value is the maximum value in histogram of image *A*. In

the first step the values of maximum bin number and its neighbors of the histogram of I_n and B_n found and compared to check if I_n has a higher peak than B_n. In the second step, histogram of the absolute difference $|I_n\text{-}B_n|$ is checked to see if most of the values accumulate near the black end.

32-bin histogram of an image will be called $H_i(.)$ where $1 \leq i \leq 32$. Both (4.9) and (4.10) are checked to find whether a camera view is covered or not.

$$\left(H_{max\,(H(I_n))-1}(I_n) + H_{max\,(H(I_n))}(I_n) + H_{max\,(H(I_n))+1}(I_n)\right) > Th_3\left(H_{max\,(H(I_n))-1}(B_n) + H_{max\,(H(I_n))}(B_n) + H_{max\,(H(I_n))+1}(B_n)\right) \quad (4.9)$$

$Th_3 > 1$ is threshold which can be increased for higher sensitivity of the algorithm. In the above equation, if a bin value is smaller than 1 or greater than 32 their corresponding value is thought as 1 or 32 respectively. As seen from Figure 15, when camera view is covered the value which is obtained by summing maximum bin number and its neighbors is greater in the histogram of I_n than in the histogram of B_n. The related bins in the histogram of I_n and B_n are represented in Figure 15.

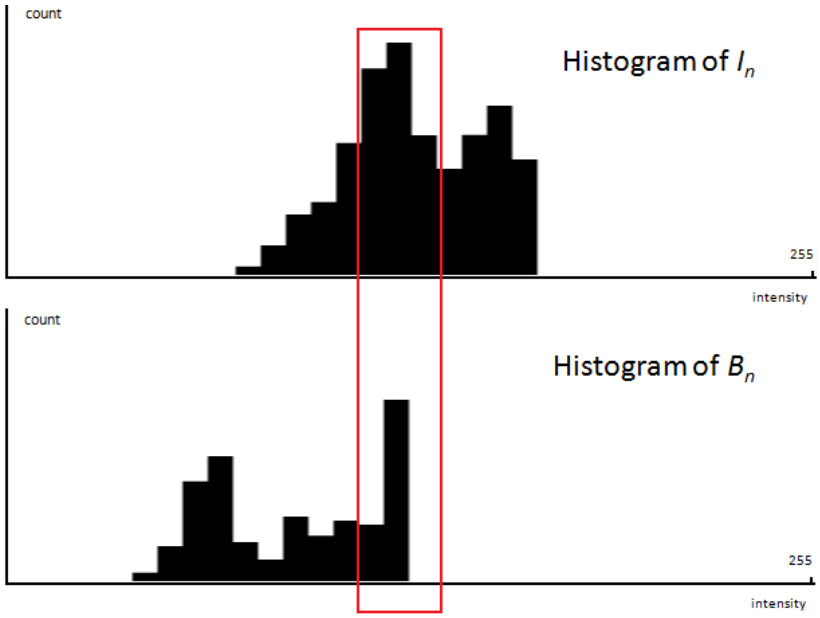

Figure 15: Maximum bin number and its neighbors of the histogram of I_n and B_n when camera view is covered

In the second step of the algorithm difference image is used. When camera view is not covered, the difference image consists of totally black pixels. In this case, all the values of the difference image's histogram are found in the first bin. If the camera covered with an object, I_n and B_n will be different from each other and the values in the difference image's histogram will expand over the histogram. Figure 16 shows the change in the histogram of difference image when camera view is covered. The second step of the algorithm is given below:

$$\sum_{i=1}^{32} H_i(|I_n - B_n|) > Th_4 \sum_{i=1}^{k} H_i(|I_n - B_n|) \quad (4.10)$$

$Th_4 > 1$ is threshold which can be increased for higher sensitivity of the algorithm. Where $0 \leq k < 32$ and when it closer to the lower bound, sensitivity will be higher, typically k=3 is found to be generating satisfactory results.

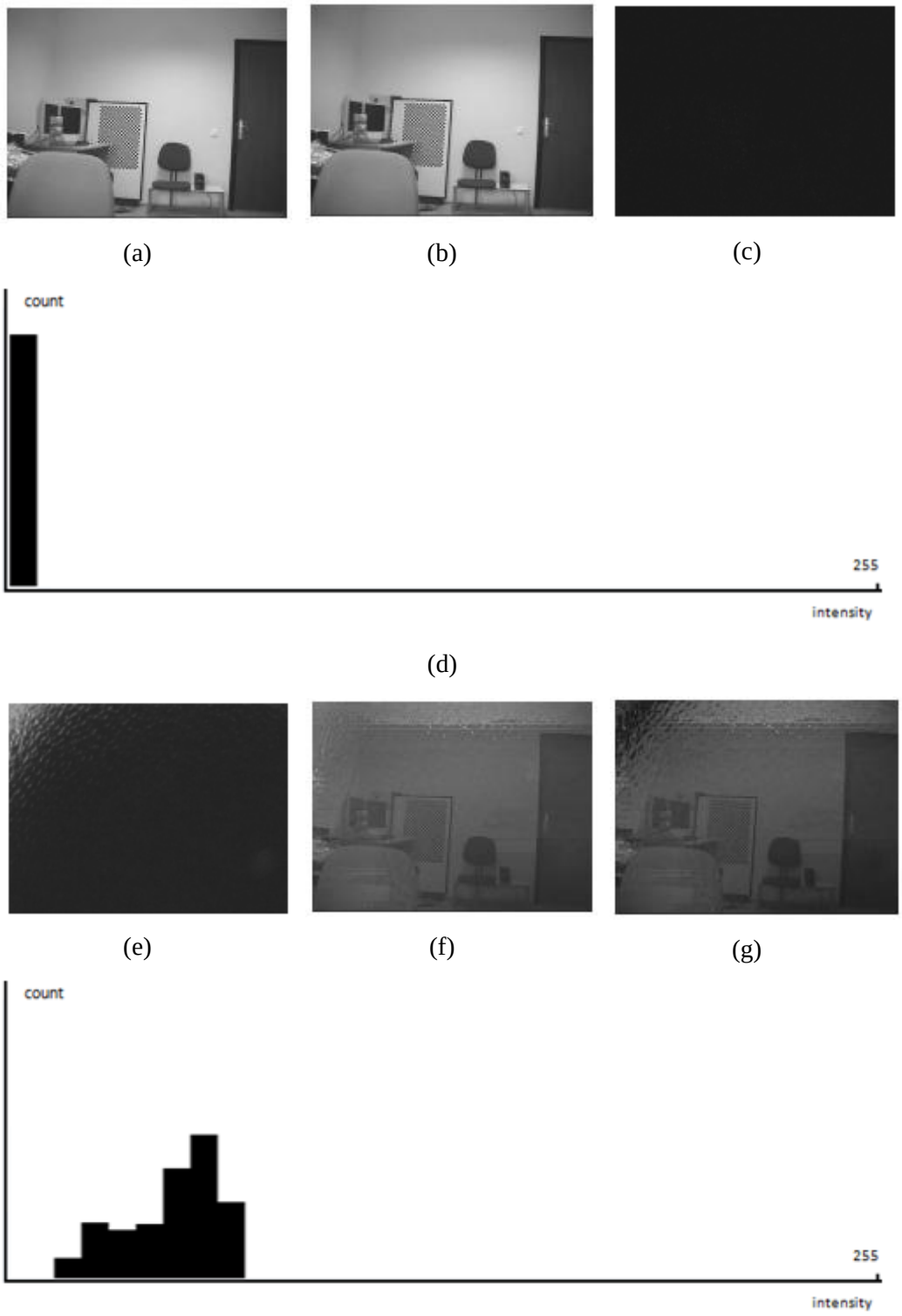

Figure 16: (a): I_n when camera view is not covered (b): B_n when camera view is not covered (c): $| I_n - B_n |$ when camera view is not covered (d): Histogram of $| I_n - B_n |$ when camera view is not covered (e): I_n when camera view is covered (f): B_n when camera view is covered (c): $| I_n - B_n |$ when camera view is covered (d): Histogram of $| I_n - B_n |$ when camera view is covered

CHAPTER 5

EXPERIMENTAL RESULTS AND COMPARISONS

5.1 Overview

We have tested the proposed algorithms in indoor and outdoor environments including real life scenarios. The proposed methods in this thesis are compared to the methods in [1-3] and the strengths and weakness of all these methods are experimentally illustrated in different test cases. In this chapter we give detailed information about the testing environment, test data, testing scenarios and results.

5.2 Testing Environment

To test the proposed methods and compare with the methods in the literature, we captured a range of images to reflect real-life camera tampering scenarios. Also to test the false alarms, we used some video sequences from the *i-LIDS dataset* [22] which contain typical surveillance scenarios without any camera tampering.

Each method explained in [2-3] is firstly implemented and tested with the same set of test videos. For [1] there is already an existing implementation and the same scenarios have been tested with this implementation. In [3], the authors propose a method which has high computational complexity. The structure used in this method is given in Figure 17. When a new image captured from the camera, it is inserted in the short term pool and the three dissimilarity measures are calculated. Assuming that, there are *m* images in the short term pool and *n* images in the long term pool. When a new image inserted in the short term pool, because each image in short term pool are compared to the images in the long term pool according to three different dissimilarity measures, *(m x n x 3)* number of calculations are required. We reduced the number of calculations by keeping the dissimilarity measures in memory and only calculating the dissimilarities for images entering the two buffers.

When a new image is inserted into the short term pool, the oldest image in the short term pool is evicted from this pool and inserted in to the long term pool. Hence, there exist 2 new images in the pools. For the new image in the short term pool, *n* number of calculations is required and for the new frame in the long term pool, *m* number of calculations is required. These calculations are done according to the three dissimilarity functions which makes the total number of calculations *3 x (m + n)* when a new image inserted into the short term pool.

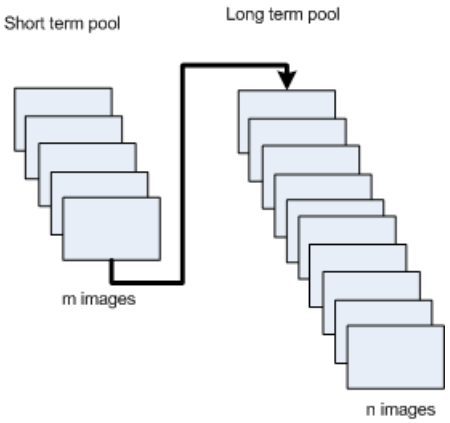

Figure 17: Incoming images are stored in the short term and long term pools

The algorithms have been implemented using C++ language and *OpenCV* library [23-24]. OpenCV is a computer vision library originally developed by Intel. OpenCV has greater than 500 algorithms, documentation and sample code for real time computer vision. This library is written in C, which makes it portable to some specific platforms. The platforms where OpenCV can run are; Microsoft Windows, Apple Mac OS X, Linux, Sony PSP[3], VCRT[4] and other embedded devices [24].

In our implementations, we needed to set some parameters regarding speed and accuracy. Because some parameters are not specified in [2, 3], we had to make some assumptions in their implementations. To speed up the algorithms, the size of the images which are captured from the camera is set to 160 x 120. Also we don't check camera tampering for all the frames. The algorithms are run once for every 20 frames. This image size and frame rate is found to be sufficient for detecting camera tampering.

[3] Play Station Portable which is a handheld game console made by Sony
[4] Real-Time OS on Smart camera: www.vision-components.com

5.3 Experimental Results

In this part, we present the test results. Tampering types which are explained in above sections are separately tested. The algorithms have been tested with the same test cases. Some images which are taken from the test scenarios are shown here to explain these cases in more detail.

5.3.1 Defocused Camera View

The algorithms were tested on a total of 27 videos having 40 defocusing events. The videos were captured in different environments and they contain a variety of test scenarios. Some of the videos are used to test false alarm cases and they don't contain any defocusing event. The algorithms are forced with the specific videos which are captured for exposing the vulnerabilities of the algorithms. Table 1 shows the results of defocused camera view tests.

Table 1: Defocused Camera Test Results for Different Algorithms

Algorithms	Number of false alarms	Number of missed events	Percentage of missed events
Aksay *et al.* [1]	5	7	17,5%
Gil-Jiménez *et al.* [2]	3	13	32,5%
Ribnick et al. [3]	4	14	35%
Proposed Method (not ignoring moving blocks)	27	6	15%
Proposed Method (ignoring moving blocks)	2	6	15%

As seen from the results, [3] gives the highest number of missed events. When we evaluated the test videos in detail we observed that if the scene contains more red and green objects the sensitivity of this algorithm increases. Since it uses red and green values to construct a 2-dimensional histogram and this histogram is used for image dissimilarity measurement, red and green objects in the scene affect the results positively. In Figure 18, 4 different red and green values 2D histogram are showed. The two images which are in the first horizontal group of the figure belong to a scene where there are small amount of red and green values. Figure 18 (a) corresponds to the non tampering case of the scene where there is lack of red and green values. If the scene is defocused, the 2D histogram doesn't change significantly as seen from the Figure 18 (b). However, if the scene contains large amount of red and green values, defocusing lens of the camera will change the 2D histogram remarkably. Figure 18 (c)

belongs to a scene which has red and green objects. When its corresponding scene defocused, the 2D histogram will change as seen in Figure 18 (d). As you see from these histograms, the change in this scene is much more than the first scene.

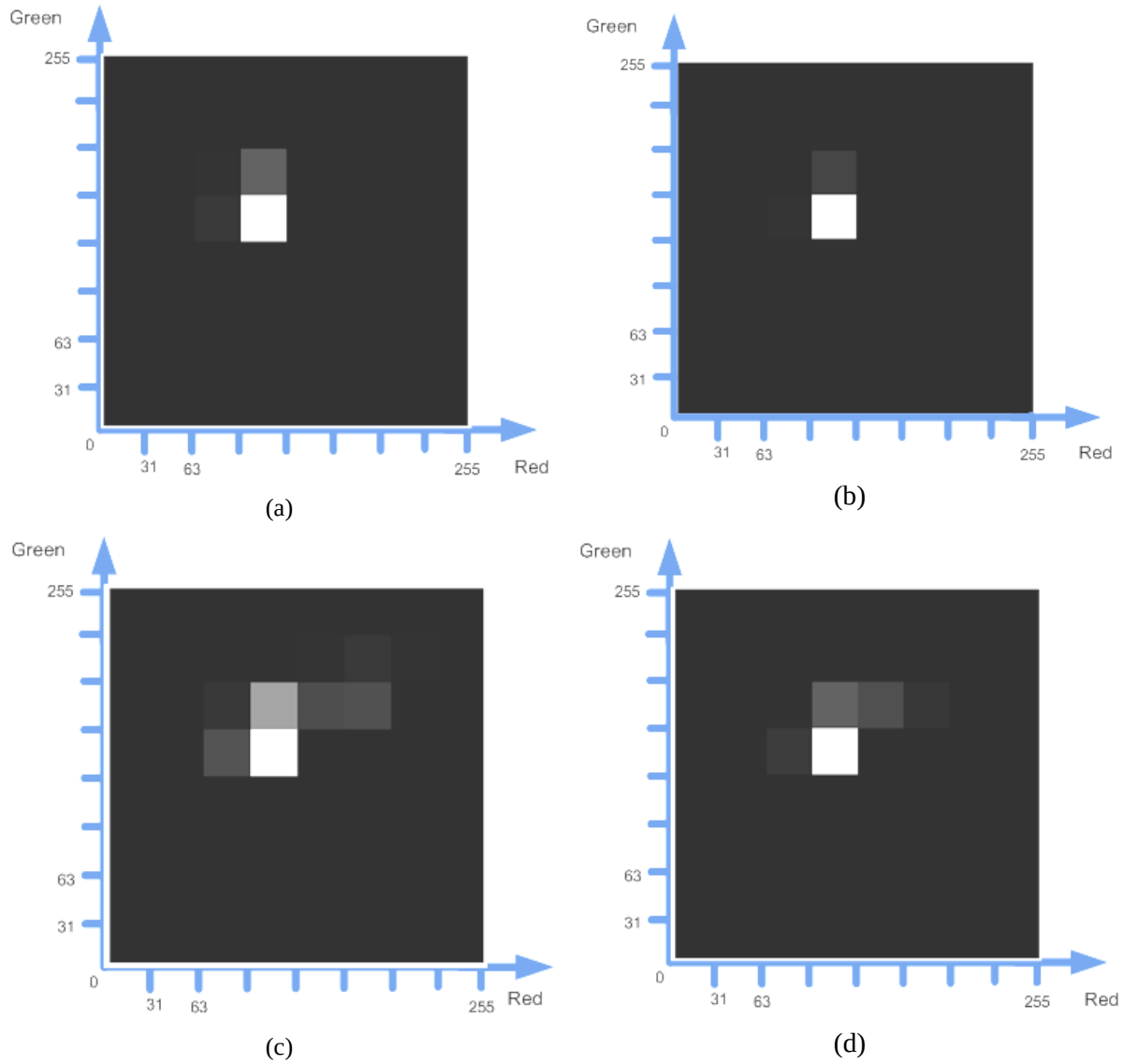

Figure 18: (a): 2D red-green values histogram of a non defocused scene which contains less amount of red and green values (b): 2D red-green values histogram of a defocused scene which contains less amount of red and green values (c): 2D red-green values histogram of a non defocused scene which contains large amount of red and green values (d): 2D red-green values histogram of a defocused scene which contains large amount of red and green values

When camera view is defocused, results of other dissimilarity functions used in [3] do not differ sufficiently enough to detect this type of tampering. Even though the number of false alarms detected by this method is not high, moving red or green objects potentially cause false alarms. When red or green objects enter or leave the scene, the result of the 2D histogram changes significantly. This significant change in the 2D histogram might result in false alarm detection.

The method in [3] compares all the images in short term and long term pools which are explained in chapter 3, when a new image captured from the camera. The medians of all these comparisons are checked to see if they exceed a certain threshold. When a camera view is defocused, it takes some time for it to affect the median of the comparisons. Therefore, this method detects tampering with some delay -in the order of a few seconds-, after the event occurred. Another important thing to mention is the fixed thresholds in this method. The authors mention that the thresholds are tuned for optimal performance based on a set of training videos. However, there is no optimal threshold for all the cases and the threshold needs to be modified for different scenes. For this type of tampering, thresholds may be adaptive according to the amount of red and green values in the scene.

In [1], W_{LH}, W_{HL}, and W_{HH} sub bands in wavelet domain are used to detect defocused camera view. These sub bands represent the horizontal, vertical and diagonal details of the image respectively. As seen from the test results, this method interprets some non tampering events as defocused camera view. In this method, moving objects bring some detail to the sub bands used to identify defocused camera view. Also, moving objects, when they move out of the scene, remove some detail from these sub bands. This is interpreted as reduction in high frequency content and results in false alarms. All the false alarms related to this method are observed to be due to the moving objects.

In [2], an edge based background model is used and to detect defocused camera view the edges in this background model is compared to the edges in the current image. Defocusing the lens of a camera causes degradation of edges in the current image and in this situation the number of edges in the background image will be higher than the number of edges in the current image. However, in real life there are moving objects in front of the camera and they change the number of edges in the current image. Even if the camera is not defocused, the number of edges in the current image may be less than the number of edges in the background image when some objects leave the scene. Some test cases have demonstrated this weakness of this method. For example, in Figure 19, a person is studying at a desk at time t_0. At that time, the current edge image and the background edge image has nearly the same number of edges. At time t_1, the person leaves the desk and as seen from the images, the number of edges in the current image is decreased. In this case, the method incorrectly identifies a defocused camera view tampering.

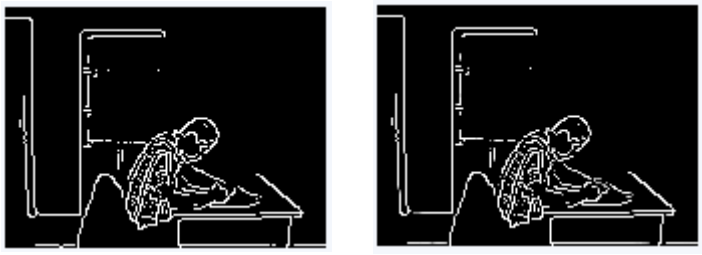

(a) (b)

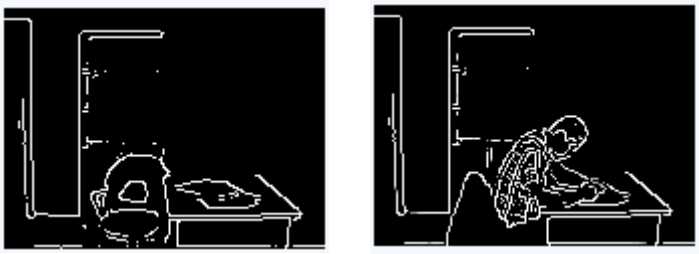

(c) (d)

Figure 19: (a): Current edge image at time t_0 (b): Background edge image at time t_0 (c): Current edge image at time t_1 (d): Background edge image at time t_1

Background image is updated to ensure that the edges of moving objects are not included in the background image [2]. There are some cases that the stationary pixels which are positioned behind the moving objects are not seen in the background image. In such cases, tampering events may be missed because the number of edges is less than the current image. For example, a scenario is given in Figure 20 from the test cases. In this case a person is walking in front of the bookshelf. As seen from Figure 20 (b) the edges of the bookshelf and the person are seen in the current edge image. However edges of the person and some edges of the bookshelf are not seen in Figure 20 (c) which represents the background edge image. In this method, the edges of the background image are taken from non moving objects and the objects which are seen on a certain number of consecutive frames. Because the person is moving and preventing some edges of the bookshelf to be seen, background image has fewer edges. If the camera is defocused in this situation, this method cannot detect the sabotage.

(a) (b) (c)

Figure 20: (a): Current image (b): Current edge image (c): Background edge image

Our first method which doesn't ignore the moving parts on the images gives a high number of false

alarms. Because moving objects on the scene changes the high frequency content in the current image, false alarms may arise. In this method high frequency content of the current and the background image is compared to detect defocused camera view. When an object enters the scene, because of its edges, it brings high frequency data to the current image. Similarly, an object leaving the scene, it causes reduction in the high frequency data in the current image. In Figure 21, a car is seen in both current and background image at time t_0. The edges of the car correspond to high frequency data in frequency domain. When the car leaves at time t_1, the high frequency data of the car disappears from the current image. Because the total amount of high frequency data decreases in the current image at time t_1, a false alarm is triggered by this method.

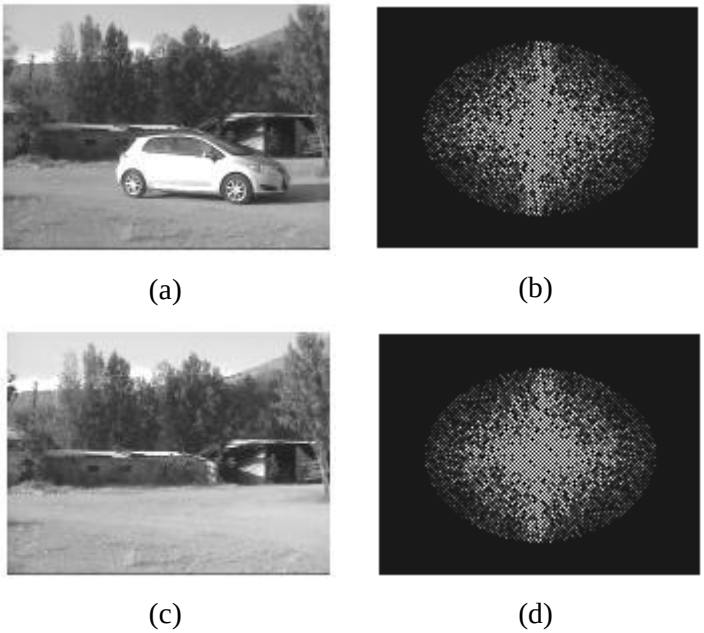

Figure 21: (a): Current image at time t_0 (b): magnitude image of current image after filtering with a Gaussian window at time t_0 (c): current image at time t_1 (d): magnitude image of current image after filtering with a Gaussian window at time t_1

Ignoring the moving blocks reduces the false alarm rate while not affecting the true alarm rate. In this method, only the blocks which don't contain any moving object are used to calculate the high frequency data of the current and the background image. If we examine the same test case as in the previous method, the blocks where the car passes through will be ignored. FFT operation is done for other blocks of the current and background image and a Gaussian windowing function is applied to each of these blocks to discriminate high frequency data. In current and background image high frequency data of the blocks which are not ignored are summed to calculate total high frequency data. After that the total high frequency values are compared to check whether the camera view is defocused. Figure 22 shows the ignored blocks when the car in the previous example moves. Figure 22 (c) shows the 8x8 pixel blocks which contain moving objects and hence, will be ignored by this method. In this image, the ignored blocks are shown with black rectangles.

(a) (b) (c)

Figure 22: (a): Current image (b): Background image (c): Ignored blocks

In this method, sometimes the defocused regions in the images are misinterpreted as moving and hence taken out of consideration. This has caused missed events in the test cases. Generally, not all the defocused blocks are interpreted as moving and the non ignoring blocks are mostly sufficient to detect defocused camera view.

Another important thing to note is the level of detail in the scene. Lack of salient edges makes the detection difficult for all of the methods. To overcome this problem, we update the thresholds adaptively according to the level of detail in background image. As explained in section 4.2, if the scene contains less level of detail, we increase the thresholds to increase the sensitivity. If it contains high level of detail, we set the threshold to a value which is closer to lower bound to prevent from potential false alarms.

The test cases include sudden illumination changes which have caused false alarms. Sudden illumination changes results in alteration in the high frequency content of the current image, while not affecting background image's high frequency content. Because the background image slowly updates, sudden illumination changes cause the current image to be significantly different from the background image. In Figure 23, change in high frequency component of the current image is showed when sudden illumination change is occurred. As seen from the images which are captured from a camera and their corresponding high frequency values, when the light in the room is turned off, high frequency content in the current image decreased because of the edges which become invisible.

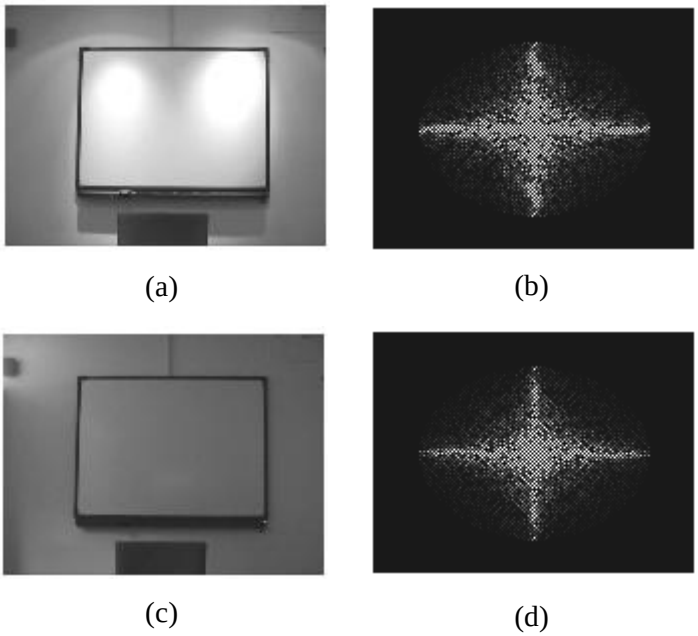

Figure 23: (a): Current image at time t_0 (b): Magnitude image of image (a) after filtering with a Gaussian window (c): Current image at time t_1 where illumination change has occurred (d): Magnitude image of image (c) after filtering with a Gaussian window

Large objects moving in front of the camera and covering the most of the view have also caused false alarms. Considering the placement of CCTV cameras, this is not a likely scenario in real world. However there are some cases which include large moving objects in front of the camera and in these test cases our firstly proposed algorithm generates false alarms. High frequency content of the images is affected by moving objects.

5.3.2 Moved Camera

We used a total of 15 video sequences containing 20 moved camera scenarios. Some of the videos don't contain any tampering event. They are used to test false alarm cases. These videos are captured in different environments with different light conditions. The results are summarized in Table 2.

As explained in the chapter 3, [1] doesn't provide a method for detecting moved camera and hence we weren't able to include in this experiment. Because moving objects in the scene changes, the result of Zero-mean Normal Cross Correlation (ZNCC) in [2], calculated correlation between the previously captured image and the current image, is lower and this results in false alarms when there is high activity.

Table 2: Moved Camera Test Results for Different Algorithms

Algorithms	Number of false alarms	Number of missed events	Percentage of missed events
Gil-Jiménez *et al.* [2]	3	7	35%
Ribnick *et al.* [3]	4	6	30%
Proposed Method	1	2	10%

In Figure 24 a person is moving in front of the camera and this causes the current image to be not matched with the previous image. The method tries to match current and the previous image and when the scene contains moving objects the correlation between current and the previous images reduces, resulting in a false alarm.

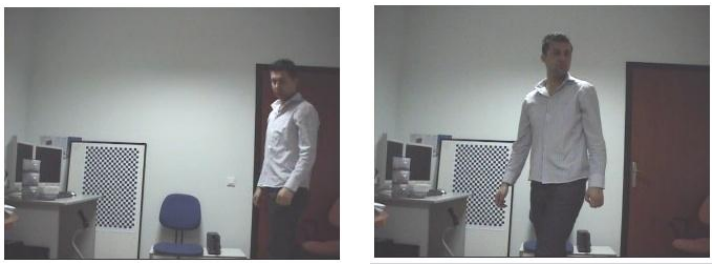

(a) (b)

Figure 24: (a): captured image at time t_0 when there are moving objects in the scene (b): captured image at time t_1 when there are moving objects in the scene

To speed up the algorithm, the method in [2] calculates ZNCC only for the pixel locations where the background image has edges. There are some cases that the edges in the background image start being updated due to small shaking of the camera. At that time, old edges in the background image slowly disappears and the edges in the new scene start to come out. In some test cases, this condition has occurred and this resulted in missed events. Lack of edges in the background image could also cause missed events. Because a type of block matching algorithm is used in this method, if there is high correlation between current and previously captured images, the method cannot find the tampering event.

The method which is proposed in [3] uses three different dissimilarity functions to detect camera tampering. Moved camera can be detected by all these three dissimilarity functions. First dissimilarity function uses a 2D histogram where the two axes display red and green values. When a camera is moved to point to a different direction, the red and green values in the new scene may be significantly different from the previous scene. In this situation, moved camera case is detected by this dissimilarity

function. There are some cases in the test scenarios which are detected by this way. In the second dissimilarity function, another 2D histogram calculation is done. This histogram is sensitive to illumination changes. Mostly, moved camera view isn't detected by this function but, some of the false alarms observed to be caused by this function. The last dissimilarity function uses a one dimensional histogram where the values are calculated according to the gradient direction of the pixels. This function is used to detect some moved camera tampering cases. When camera view is moved, some of the pixels in the scene are seen as moving and the histogram differs significantly.

In the proposed method, we compare the background image to a delayed background image to detect the moved camera view. When a camera is moved to reflect a different view, the background starts to update. If the difference between the updated background and the delayed background is higher than a threshold, an alarm is triggered by this method to indicate the movement of the camera. There are some cases that moving objects enter to or leave the adaptive background image. In these cases, the background image will be different than the delayed background image, and if the amount of difference is greater than the threshold a false alarm is generated. In Figure 25, a person is studying in the scene at time t_0 and because he is in the scene for several minutes, he is also seen in the background image and in the delayed background image. When he leaves the scene, the background image starts updating. At time t_1, the person disappears from the background image. At this time, background image is different than the delayed background image. Our method doesn't generate false alarm for this case because the difference between background and delayed background image is not enough for an alarm. However, if the moving object covers most of the view, which is not a likely scenario in real life, or if the sensitivity increased by updating the threshold, a false alarm could be raised by this method.

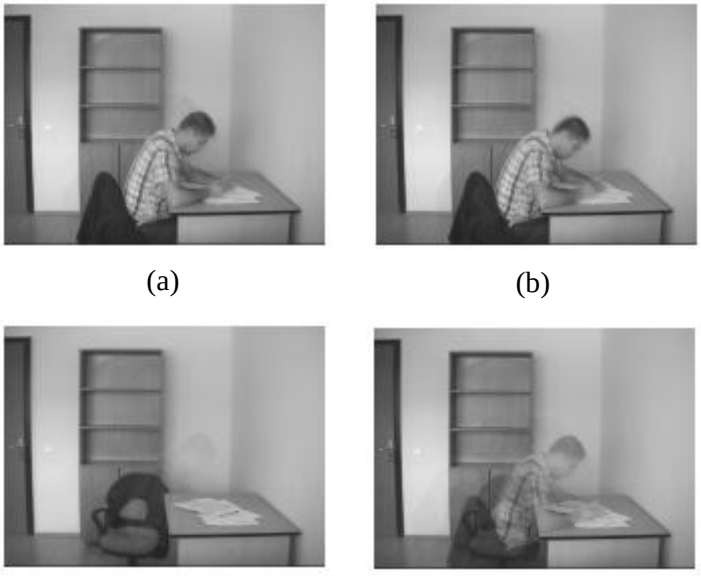

(a) (b)

(c) (d)

Figure 25: (a): Background image at time t_0 (b): Delayed background image at time t_0 (c): Background image at time t_1 (b): Delayed background image at time t_1

Lack of edges in the view makes the detection difficult for our method. If the view has large amount of uniform areas and if it is changed to a similar view by moving the camera, detection of tampering becomes difficult. As explained in section 4.4, to overcome this problem, we update the threshold adaptively according to the level of detail in background image. In this case, sensitivity is increased by setting the threshold to a value which is closer to 0.

5.3.3 Covered Camera View

We used a total of 30 video sequences having 42 covered camera view cases. The results of the algorithms are summarized in Table 3. The test videos are captured in different environments and they reflect real life scenarios. Not all the videos include tampering; some of them are used to test false alarm cases. In these videos the view is covered with different objects to see the effect of the covering object to the performance of these methods.

Table 3: Covered Camera Test Results for Different Algorithms

Algorithms	Number of false alarms	Number of missed events	Percentage of missed events
Aksay *et al.* [1]	7	7	16,7%
Gil-Jiménez *et al.* [2]	14	5	11,9%
Gil-Jiménez *et al.* [2] *(block based)*	28	0	0%
Ribnick *et al.* [3]	10	3	7,1%
Proposed Method	4	2	4,8%

In [2], an entropy value is calculated and low entropy values are used to infer covered camera view. When an object covers the lens of the camera, the objects in the scene will no longer be visible, and the pixels in the background image disappear. In this situation, the proportion of black pixels in the background image increases. In Figure 26, we show the background image and the change in the entropy of this background image over time when the camera view is covered. In Figure 26(a), the background image at time t_0 is showed where the camera view is not covered. As you see from the graphic, the entropy value is higher at time t_0. When the camera view is covered at time t_1 which is shown in Figure 26(b), the edges in the background image starts disappearing. Loss of edges in the background image causes the entropy value to decrease.

Moving objects which are covering the edges in the background image has caused false alarms. Such objects change the pixels in the background image and the entropy is affected. The method in [2] also has an alternative method for partial camera occlusions. In this method, image is divided into blocks and entropy is calculated for each block separately. If one of the entropy values is lower than previously calculated entropy, an alarm is triggered. Even though this increases the true alarm detection rate, as the entropy of individual blocks are affected significantly by moving objects, it generates considerably more false alarms and has the highest false alarm rate.

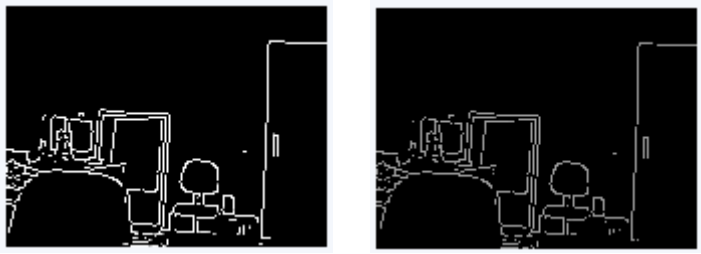

(a) (b)

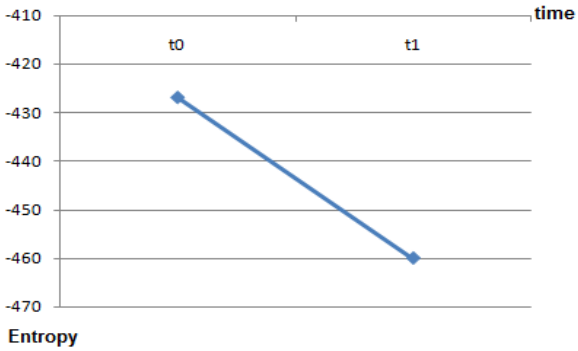

(c)

Figure 26: (a): Background image which belongs to a non covered view at time t_0 (b): Background image of the covered view at time t_1 (c): Entropy graphic

As we explain in section 4.4, we use a method similar to the one proposed in [1] with some modifications. As seen from the results, the false alarm rate is lower in the proposed method than this method. This method compares the maximum values of the histograms which are calculated using the current and background image. However, there have been some test cases that an object enters the scene and the maximum value in the current image's histogram significantly differs. In these cases, false alarms are generated by this method.

The method in [3] uses 2 functions to detect covered camera view. When a camera view is covered, the red and green objects in the scene become invisible. This change in the scene causes the 2D red and green values histogram to change significantly. The first function in this method is used to detect covered camera view. Another function which is used to detect this type of tampering is histogram L1R difference. In this function another 2D histogram is calculated which is sensitive to changes in illumination. Because the illumination in the scene changes when camera view is covered, this function detects tampering. Figure 27 shows the change of these 2D histograms when the camera view is covered.

Because the histograms in method [3] are sensitive to color and illumination changes, moving objects in front of the camera and some illumination changes caused by sun light flickers are marked as camera tampering. False alarms which are generated by this method are caused by these conditions.

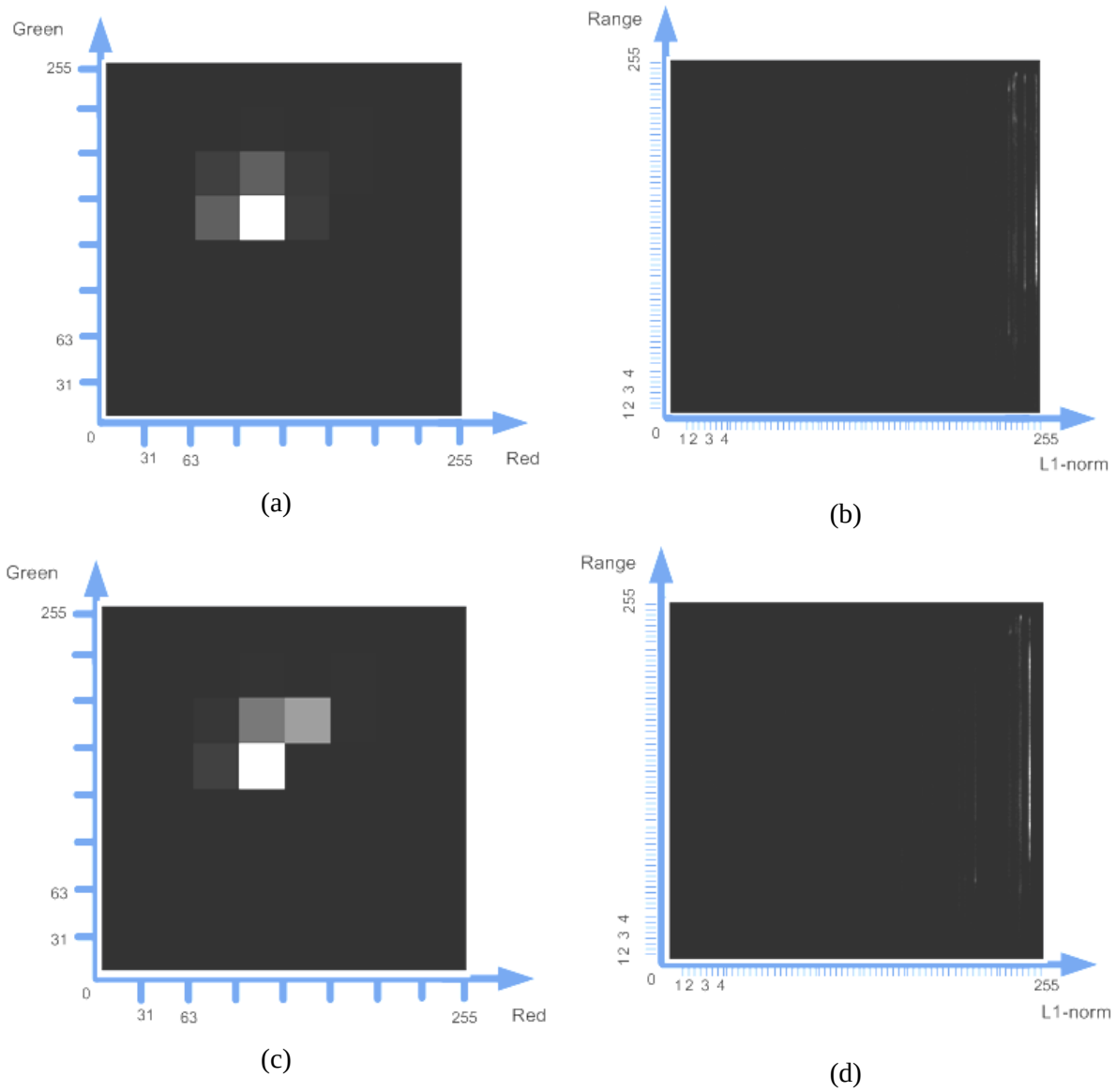

Figure 27: (a): 2D red and green values of non covered view (b): 2D L1R histogram of non covered view (c): 2D red and green values of covered view (d): 2D L1R histogram of covered view

We propose a method which uses intensity histograms of the current and background images to detect covered camera view. The method has two steps. In the first step, we compare the maximum value bin of the current image's histogram along with its neighbors to the same bins in the background image's histogram. After that, we check the bins in the histogram of the difference image which is obtained by calculating absolute difference of the pixels in current image and background image. If these two steps are satisfied according to the equations (4.9, 4.10), the method raises an alarm. Figure 28 shows the histograms of current image, background image and the difference image.

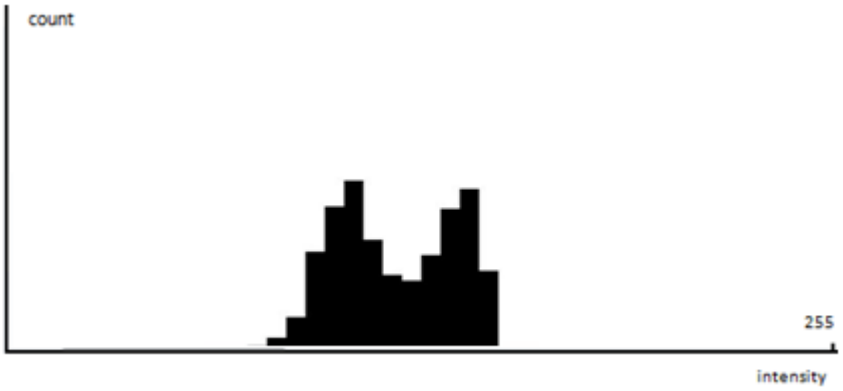

(a)

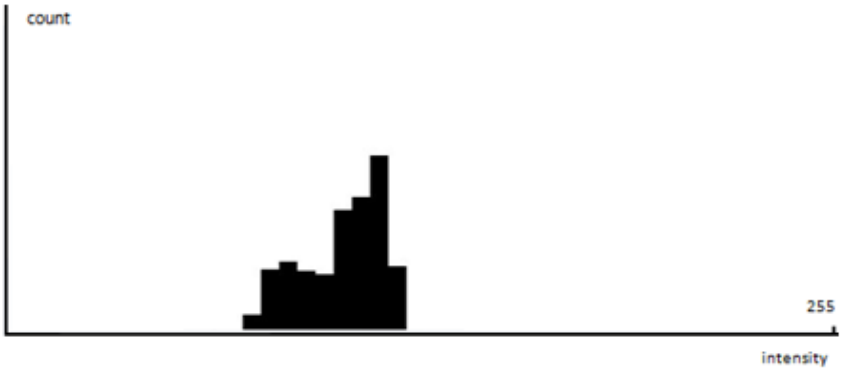

(b)

(c)

Figure 28: (a): Histogram of current image when camera view is covered (b): histogram of background image when camera view is covered (c): histogram of difference image when camera view is covered

In this method, sudden illumination changes in the scene modify the difference image significantly and in some test cases this has raised false alarms. Moving objects which are covering the most part of the view has also caused false alarms. These are the cases where the proposed method could generate false alarms.

Sudden illumination changes are a shortcoming of our camera tampering detection algorithms. The performances of these algorithms are affected when the amount of light in the environment changes suddenly. Our test cases include this kind of events and in these test cases we see many false alarms and a few missed events. To overcome this problem, an edge correspondence check may be applied. Edge correspondence check is used to check that if a camera still is or is not monitoring the same scene. If a camera viewing the same scene the edges in the background image and in the current images should be in the same locations. If a sudden illumination change is occurred, camera still views the same scene. By confirming that the camera is viewing the same scene we can distinguish tampering cases from sudden illumination changes. To find number of corresponding edge pixels, we can use the following equation.

$$E_{corresponding} = \begin{cases} E_{corresponding} + 1 & , if\ |I_n(x,y) - B_n(x,y)| < Th_5 \\ E_{corresponding} & , if\ |I_n(x,y) - B_n(x,y)| \geq Th_5 \end{cases} \quad (5.1)$$

where $E_{corresponding}$ is the number of corresponding edge pixels. *(x,y)* is the pixel positions where edges exist in the current image and $Th_5 > 1$ is the threshold value. When Th_5 is set to a value which is closer to one the sensitivity is increased. After finding the number of corresponding edge pixels, we may use the following equation to find whether the camera is viewing the same scene or not.

$$E_{corresponding} > Th_6 E_{total} \quad (5.2)$$

In this equation E_{total} is the number of pixels where there are edges in the current image and $0<Th_6<1$ is the threshold value. To increase the sensitivity we set the threshold value which is closer to 1.

Another method which may be applied to reduce false alarm rate when sudden illumination change is occurred may be normalizing all the pixels of the images according to the average light in the images. If we subtract a proportion of average pixel value from all the pixels, the values of the pixels in the images will be similar when a sudden illumination change is occurred. When the level of light in the images is high or low, normalized images will be very similar. Because these normalized images is more stable against sudden illumination changes, the number of false alarms or missed events may be reduced by using these images in the camera tampering detection algorithms. This process can be thought as preprocessing of camera tampering detection algorithms and it is showed in the following equation:

$$I_{normalized}\ (x,y) = I_{(x,y)} - P\mu \quad (5.3)$$

where $I_{normalized}(x,y)$ is the normalized pixel value at pixel position (x,y), and $I_{(x,y)}$ is the pixel value of input image at position (x,y). μ is the mean pixel value of image I and P is the proportion value.

CHAPTER 6

CONCLUSIONS AND FUTURE WORK

In this thesis, we propose new algorithms to detect three types of camera tampering which are camera defocusing, camera movement and covering of a camera view. The algorithms are based on an adaptive background estimation technique which uses a threshold mechanism to identify moving objects. The thresholds are adaptively updated over time in accordance with the moving pixels in the scene. For detecting defocused camera view, high frequency components of current image and background image are compared. When camera view is defocused, the edges in the current image are degraded which decreases the high frequency components of the current image. To acquire high frequency components of the images, Fourier transform is applied to the images and then a Gaussian window is used to discriminate high frequency values from the low frequencies. While we experimenting this method, we realized that the moving objects in the scene can significantly change high frequency data of current image which results in false alarm. To overcome this problem, we propose an extension of this method which calculates high frequency data for only non moving regions in the current and background image. For camera moving, we propose a method which compares the background image to a delayed background image and the number of different pixels is used to determine whether the camera is moved to a different direction. For camera covering, we propose a method which checks the histograms of current, background and difference image. The difference image is obtained by taking absolute difference between current and background image. In the first step of this method, we compare the maximum value bin of the current image's histogram along with its neighbors to the same bins in the background image's histogram. In the second step of the method, the values in the histogram of difference image are analyzed to check whether or not a significant percentage of the values are located near the black end.

We evaluated the proposed algorithms using a variety of camera tampering scenarios as well as 4 typical video surveillance footages not containing any tampering events totaling approximately 14 minutes from *i-LIDS dataset* [22]. Our results show that the proposed methods have low false alarm

rates and more favorable true alarm rates in defocused camera view, moved camera and covered camera view cases compared to the other algorithms. In the defocused camera case, 2 different methods are proposed. Both methods have missed same tampering events, but the first one generates significant number of false alarms while the second one generates fewer false alarms. We have decreased the number false alarms by block based processing to account for moving objects in the scene.

The test videos include few sudden illumination changes which could potentially cause false alarms. Even though not a likely scenario -considering the placement of real life CCTV cameras-, large objects moving in front of the camera and covering most of the view could increase the number of false alarms.

All the methods which aim to detect tampered camera view based on the same approach that, newly captured images are compared to the older ones and if there is significant difference an alarm case is generated. In this study, we also based on the same approach and proposed new techniques for detecting camera tampering. We have evaluated our approach with a set of videos and compared to the other methods in the literature. As seen from the test results, false alarm rate and number of missed tampering events is lower than the other methods. We hope that this study will help researchers to develop new solutions to similar problems in video surveillance research area.

In the future, the proposed camera tampering detection algorithms may be enhanced by making them robust against sudden illumination changes. In Chapter 5 some methods which may be used reduce effect of sudden illumination changes are explained. These methods may be implemented and tested to evaluate their performance.

These algorithms may be adapted to work in different platforms in the future. For example, the algorithms may work in embedded systems and by this way, all the checks against camera tampering may work on a single camera. This system may also be integrated into existing security systems. For example, referring to the Mexico prison escape which is explained in chapter 1, if there had been an integrated system where the camera tampering detection algorithms controlled the doors of that section of the prison, the doors would be able to be lock automatically and the escape may have been prevented.

REFERENCES

[1] Aksay Anıl, Temizel Alptekin and Çetin A. Enis., "Camera Tamper Detection Using Wavelet Analysis for Video Surveillance." IEEE International Conferance on Video and Signal Based Surveillance, September 2007.

[2] Gil-Jiménez P., Lopez-Sastre R., Siegmann P., Acevedo-Rodriguez J., Maldonado-Bascon S., "Automatic Control of Video Surveillance Camera Sabotage." s.l. : J. Mira and J.R. Alvarez (Eds.): IWINAC 2007, 2007.

[3] Ribnick Evan, Atev Stefan, Masoud Osama, Papanikolopoulos Nikolas, Voyles Richard, "Real-Time Detection of Camera Tampering." s.l. : IEEE International Conferance on Video and Signal Based Surveliance, 2006.

[4] Piccardi, Massimo., "Background Subtraction Techniques: a review." s.l. : IEEE International Conference on Systems, Man and Cybernetics, 2004. 0-7803-8566.

[5] Sen-Ching, S. Cheung and Chandrika, Kamath., "Robust techniques for background subtraction in urban traffic video." San Jose : Video Communications and Image Processing, SPIE Electronic Imaging, January 2004. UCRL-JC-153846-ABS, UCRL-CONF-200706 .

[6] Wren, C., Azarhayejani, A., Darrell, T. A.P., "Pfinder: real-time tracking of the human." s.l. : IEEE Trans. on Patfern Anal. and Machine Intell. vol. 19, no. 7, pp. 78g785, 1997.

[7] , Background subtraction, part 1: MATLAB models. *DSP DesignLine.* [Online] [Cited: 12 May 2009.] http://www.dspdesignline.com/howto/210000460;jsessionid=KGBUUEXZDIKJ0QSNDLRCKHSCJUNN2JVN?pgno=3.

[8] Stauffer, C. and Grimson, W.E.L., "Adaptive background mixture models for real-time tracking." s.l. : IEEE CVPR 1999, pp. 24&252, June 1999.

[9] Elgammal, A., Harwood, D. and Davis, L.S., "Non parametric model for background subtraction." June 2000. Proc. ECCV 2000. pp. 751-767.

[10] Han, Bohyung, Comaniciu, Dorin and Davis, Larry., "Sequential Kernel Density Approximation Through Mode Propagation:applications to background modelling." January 2004. Proc. Asian Conf. on Computer Vision.

[11] Seki, Makito, et al., "Background Subtraction based on Cooccurrence of Image Variations." 2003. IEEE Computer Society Conference on Computer Vision and Pattern Recognition (CVPR'03), 1063-6919/03. pp. 65-72.

[12] Xu, Zhifei, Shi, Pengfei and Yu-Hua Gu, Irene., "An Eigenbackground Subtraction Method Using Recursive Error Compensation." [book auth.] Lecture Notes in Computer Science. *Advances in Multimedia Information Processing - PCM 2006.* s.l. : Springer Berlin / Heidelberg, 2006, pp. 779-787.

[13] Collins R.T., Lipton A.J., Kanade T., Fujiyoshi H., Duggins D., Tsin Y., Tolliver D., Enomoto N., Hasegawa O., Burt P., Wixon L., *A system for video surveillance and monitoring: VSAM final report.* s.l. : Carnegie Mellon University, May 1998. Technical Report CMURI-TR-00-12.

[14] Fridrich, Jiri., "Image Watermarking for Tamper Detection." 1998. Proc. of ICIP, vol.2. pp. 404-408.

[15] Roberts, D.K., "Security Camera Video Authentication." October 2002. Digital Signal Processing Workshop and the Signal Processing Education Workshop. pp. 125-130.

[16] Lim, Suk Hwan, Yen, Jonathan and Wu, Peng., "DETECTION OF OUT-OF-FOCUS DIGITAL PHOTOGRAPHS." January 2005. Imaging Systems Laboratory, HP Laboratories Palo Alto.

[17] Nam, Jeho and Tewfik, Ahmed H., "Detection of Gradual Transitions in Video Sequences." August 2005. IEEE TRANSACTIONS ON MULTIMEDIA, VOL. 7, NO. 4. pp. 667-679.

[18] Heng, Wei Jyh and Ngan, King N., "Integrated Shot Boundary Detection using Object-based Technique." October 1999. Proceedings of International Conference on Image Processing, vol. 3. pp. 289-293.

[19] Tomassi, Carlo and Kanade, Takeo., "Shape and Motion from Image Image Streams Under Orthography: a Factorization Method." September 1993. IJCP, vol. 9, no. 2. pp. 864-884.

[20] Weng, Juyang, Ahuja, Narendra and Huang, Thomas S., "Optimal Motion and Structure Estimation." September 1993. IEEE TRANSACTIONS ON PATTERN ANALYSIS AND MACHINE INTELLIGENCE, VOL. 15, NO. 9. pp. 864-884.

[21] Harasse, S., Bonnaud, L., Caplier, A., Desvignes, M., "Automated camera dysfunctions detection." March 2004. Image Analysis and Interpretation, 6th IEEE Southwest Symposium. pp. 36-40.

[22] i-LIDS dataset for AVSS 2007. [Online] [Cited: 13 March 2009.] http://www.elec.qmul.ac.uk/staffinfo/andrea/avss2007_d.html.

[23] *OpenCV Documentation and FAQs.* [Online] [Cited: 13 March 2009.] http://opencvlibrary.sourceforge.net/.

[24] Gary, Bradski and Kaehler Adrian., *Learning OpenCV.* s.l. : O'Reilly, September 2008. 978-0-596-51613-0.